https://doi.org/10.5194/egusphere-2026-4655
Preprint. Discussion started: 12 August 2026

An Open-Source Python Framework for the Flexible Deployment and Advanced Applications of the Variable Infiltration Capacity (VIC) Model

Xudong Zheng[1], Dengfeng Liu[1], Qiuhong Tang[2], Qiang Li[3], Haoyu Liao[4], Hao Wang[5]

[1]State Key Laboratory of Water Engineering Ecology and Environment in Arid Area, Xi'an University of Technology, Xi'an, 710048, China
[2]Department of Earth System Science, Tsinghua University, 100084, Beijing, China.
[3]College of Forestry, Northwest A&F University, Yangling, 712100, China
[4]Shaanxi Provincial Water Conservancy and Hydropower Development Center, Department of Water Resources of Shaanxi Province, Xi'an, 710004, China
[5]State Key Laboratory of Simulation and Regulation of Water Cycle in River Basin, China Institute of Water Resources and Hydropower Research, Beijing, 100038, China

Correspondence to: Dengfeng. Liu（liudf@xaut.edu.cn)

https://doi.org/10.5194/egusphere-2026-4655
Preprint. Discussion started: 12 August 2026

Abstract. The development of the Variable Infiltration Capacity (VIC) model to version 5 has endowed it with enhanced land-surface-modelling features, establishing it as a modern and cutting-edge tool for hydrological research. However, its adoption is limited by challenges in complex data processing and parameter preparation. To address this issue, this study proposes the Easy VIC Build (EVB) framework, an open-source Python package with an object-oriented, modular design, developed for efficient and flexible VIC deployment. Two real-world basin setups were selected for model application to validate the effectiveness of the EVB framework. The results indicate that, based on the EVB framework, reliable spatial parameters with robust transferability can be derived, while VIC models can be conveniently deployed and achieve satisfactory simulation performance. The EVB framework provides a well-suited workbench for advanced applications of the VIC model, promising to further leverage the value of VIC-5 in hydrology and related fields.

1 Introduction

Enhancements in computational capabilities have alleviated the restrictions on the granularity with which natural processes can be depicted. The development of hydrological models, from conceptual lumped models to physical distributed models, over the last decade reflects this trend (Beven, 2002). As a result, the new generation of distributed hydrological models broadens the range of their application, evolving from a basic rainfall-runoff response analysis to roles in water resource management, flood risk management, and serving as the land surface models (LSMs) in the coupling framework with the general circulation models (GCMs) (Sun et al., 2023; Wang et al., 2023). Typically, the Variable Infiltration Capacity (VIC) large-scale distributed hydrological model has been refined from version 4 to 5 in the recent period. This development enhanced its LSM features, including the separation of the physical core, the division of four types of drivers (i.e., Classic, Image, CESM, and Python drivers), and its ability to use the more universal NetCDF format data for model data transfers (Hamman et al., 2018). Although the core physical mechanisms remain unchanged, this restructuring is historically significant. It prolongs the lifecycle of the VIC model, making it more suitable for modern applications and better equipped for deployment in various offline or coupled environments (Wang et al., 2024; Broman et al., 2024).

However, the complexity involved in VIC model deployment, including model configuration, preparation of input datasets, and parameter calibration, creates substantial technical barriers that restrict its expansion and advanced applications. In the current era, which is often termed the age of big data or the fourth paradigm of data-intensive science, exploring the potential of the VIC model to explain real-world phenomena through the integration of multisource data requires the accommodation of different data types and spatiotemporal scales (Peters-Lidard et al., 2017). This, in turn, presents challenges for the VIC model deployment. As a comparison, the Soil and Water Assessment Tool (SWAT) model is a prominent success story within the hydrology community. Its intuitive interface and seamless integration with Geographic Information System (GIS) have been identified as critical drivers of its widespread adoption, effectively addressing operational challenges in practical applications (Qiu et al., 2017). On the other hand, the source-code-centric architecture of the VIC model places additional

https://doi.org/10.5194/egusphere-2026-4655
Preprint. Discussion started: 12 August 2026

burdens on users by requiring independent data preprocessing and external toolkits for spatial information extraction. Such requirements increase the technical complexity of model implementation and hinder its scalability. Therefore, there is an urgent need within the community for a unified, flexible, open-source framework for VIC model deployment to facilitate its widespread application across diverse development environments and research scales.

A recent attempt in this domain has been made by Wi et al. (2017), who developed a VIC-Automated Setup Toolkit (VIC-ASSIST) in the MATLAB environment. This is a very useful tool for VIC beginners with limited programming experience, as it is designed to be “user-friendly”. However, this deployment solution lacks sufficient scalability, which can be illustrated through several aspects. Firstly, it is well known that MATLAB is a commercial software designed for professional users and is difficult for many users to access. Worse yet, it is not even a standard programming language, lacking the well-established ecosystem and programming features found in languages like Python. Secondly, to simplify usage, VIC-ASSIST enforces several fixed configurations, such as limiting the number of soil layers to three, providing only a few optional resolutions and data sources, and using predefined calibration algorithms and targets. From a design pattern perspective, this is a tightly coupled design, which significantly restricts the tool’s scalability when adapting to different requirements (Gamma et al., 1995). Finally, and perhaps most importantly, this model deployment tool lacks synchronized evolution with the development of the model itself. With VIC having evolved to version 5, it now lacks the necessary applicability.

To address the above issues, this study aims to propose an open-source, Python-based flexible framework for deploying the VIC model, specifically targeting the latest VIC-5 version. The proposed framework, called Easy VIC Build (EVB), is expected to have the following features: (1) full implementation in Python, enabling on-demand scalability within the rich Python ecosystem; (2) a loosely coupled, object-oriented programming (OOP) design that preserves the modularity of individual components, allowing for their replacement or modification without disrupting the overall architecture, for example, the model structures (e.g., soil layer depths, root zone number, etc.), data sources and processing (e.g., forcing and land surface data), and spatiotemporal scales can be adjusted as needed to align with specific research objectives; and (3) keeping up-to-date with VIC development, the framework is designed to support the processing and generation of various popular data formats, including NetCDF and TIFF. In addition, several advanced methods associated with model deployment were embedded into the EVB framework to enhance its general applicability, including the Multiscale Parameter Regionalization (MPR) and the General Unit Hydrograph (GUH) (Samaniego et al., 2010; Mizukami et al., 2017; Guo, 2022b). The EVB framework was applied across multiple modelling applications in the real-world basin system to rigorously evaluate its effectiveness. By simplifying and standardizing the deployment workflow, the proposed framework can reduce technical barriers and facilitate broader adoption of the VIC model among both existing and potential users.

The remainder of this paper is organized as follows. The design, architecture, and required environment of the EVB framework are described in Section 2. Section 3 presents its functionalities and the workflow of VIC model deployment.

https://doi.org/10.5194/egusphere-2026-4655
Preprint. Discussion started: 12 August 2026

Section 4 provides a description of the case basins and data collection, while Section 5 demonstrates several modelling applications. Finally, conclusions are provided in Section 6.

2 Framework design and environmental requirements

In this section, we present the design philosophy and basic architecture of the Easy VIC Build (EVB) framework. The required runtime environment will also be described in this section to help users with configuration.

2.1 Architecture of the EVB

Fig. 1 shows the architecture of the EVB framework. In brief, it is built on the following premises: (a) the tools subpackage, which provides foundational functions to support the core operations of other modules; (b) the workflow for VIC model deployment, along with the associated seven modules; and (c) the Evb_dir class for managing the directory structure of the generated files. Through this architecture, the EVB framework enables users to deploy the VIC model with flexibility across diverse configurations.

Here, we highlight the advantages of this architectural design, specifically its object-oriented programming and loosely coupled structure. This is achieved by decomposing various functionalities into separate classes, functions, modules, and subpackages, allowing the users to modify and extend the framework as needed at any time. Fundamentally, the proposed framework builds upon these capabilities and the underlying architecture of VIC-5, supporting NetCDF-based data flows for inputs, outputs, and parameters, the official routing extension, and multi-processing execution. These design choices are consistent with the principles of reproducibility, grouping, isolation, and sharing highlighted by Hamman et al. (2018). Below, we introduce several classes that constitute the core of the EVB architecture, along with the underlying concepts.

https://doi.org/10.5194/egusphere-2026-4655
Preprint. Discussion started: 12 August 2026

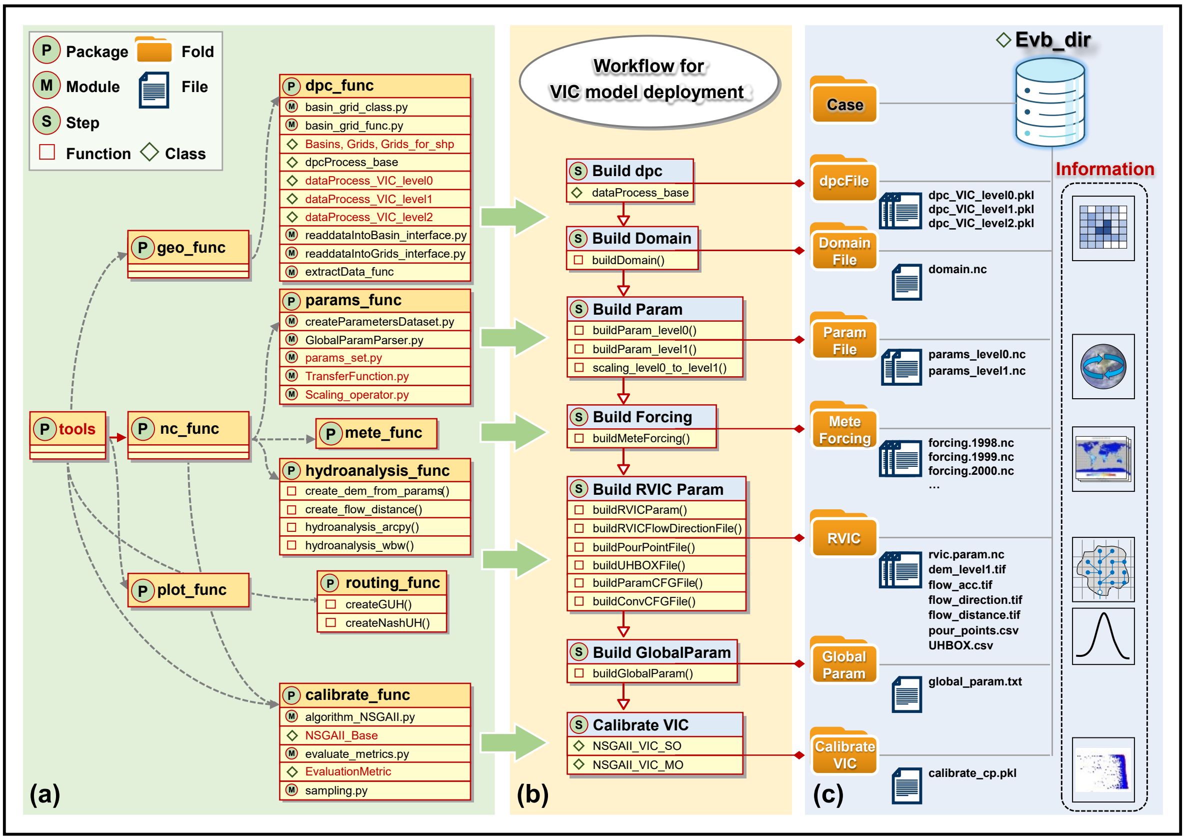

Figure 1. The architecture of the Easy VIC Build (EVB) framework. (a) The tools subpackage, along with its structure, forms the essential foundation that underpins the functionality and operation of other modules. (b) The workflow for VIC model deployment and related modules. (c) The file tree structure generated by the EVB framework, which is managed by the Evb_dir class, contains the information for the deployment of the VIC model. The core modules or classes are marked in red.

2.1.1 Two fundamental classes for geographic information: Grids and Basins

Each deployed hydrological model is intrinsically linked to a specific region (or basin) and a corresponding horizontal discretization, both of which embed spatial information that can be mapped to other information, such as soil properties. Typically, the region is represented by a shapefile within a GIS, either supplied by the user or derived through a relevant basin delineation method. Meanwhile, horizontal discretization is commonly achieved using a structured array of rectangular grids.

To enable an object-oriented representation within this framework, we constructed two subclasses, termed Basins and Grids, which inherit from the GeoDataFrame class provided by the GeoPandas package (Jordahl et al., 2020). In this way, they inherit the advantages and functionality of their parent class, such as convenient plotting and I/O (i.e., input and output) capabilities. These two subclasses provide a unified representation of the two types of geographic information mentioned above, and they act as proxies for regions and grids while sharing their geographic information throughout the model

https://doi.org/10.5194/egusphere-2026-4655
Preprint. Discussion started: 12 August 2026

deployment workflow. From an architectural design perspective, they serve as the foundation for data processing classes (hereafter dpc classes), thereby enabling interfaces for interaction with other information or data.

2.1.2 Information level division of modelling scale and the data processing classes

A hydrological model is an integration of information from multiple scales. For the VIC model, information from both finer scales (e.g., land surface information at the kilometer level) and coarser scales (e.g., meteorological forcing information at tens-of-kilometers level) must be unified to a predefined, singular modelling scale. It is essential for modelers to clearly distinguish between the scales of different information. Here, we adopt the concept proposed by Samaniego et al. (2010), who divided the spatial scales into three levels: level 0, level 1, and level 2. In brief, information at level 0 is used to describe sub-grid variability of basin characteristics at finer scales, such as topography and soil properties. Level 1 is associated with the modelling scale and represents the scale at which the primary hydrological processes are focused. Finally, level 2 corresponds to the meteorological forcing scale. Here, we further introduce a level 3 representation to capture basin scale information, such as watershed characteristics and outlet runoff. This multiscale classification facilitates the integration of information across different spatial scales and provides a basis for implementing the Multiscale Parameter Regionalization (MPR) technique. Building on the information level division, we established an abstract base class for data processing and subsequently implemented several VIC-specific subclasses, collectively refer to as dpc classes (Fig. 1a). They share a similar structure but encompass different information at diverse scales. Each dpc class contains a Basins and a Grids instance as attributes to represent geographic information at their respective scale.

2.1.3 Path management and logger class

In this systematic model deployment framework, effective path management is implemented though a class named Evb_dir. This class enables path definition and modification while automatically propagating these values throughout the entire modelling workflow. We have also implemented a Logger class to monitor and document the model deployment process, so that potential errors and performance bottlenecks during the deployment can be timely identified.

2.2 Environmental requirements

The EVB framework is fully developed in Python and entails certain basic environmental requirements. All the required environments are open-source and easily accessible. To assist users in configuration, we grouped the required environments into three categories based on their functionality: (a) basic computation and visualization, (b) geospatial data processing, and (c) optimization. Table 1 lists the names and sources of these Python packages. We also provide a pyproject.toml file in the source code, aligned with the latest Python standards, to simplify the environment setup.

https://doi.org/10.5194/egusphere-2026-4655
Preprint. Discussion started: 12 August 2026

Table 1. A summary of the EVB framework environmental requirements.

Category	Package Name	Functionality	Reference	Source
Basic computation and visualization	NumPy	Arrays and operations	Harris et al. (2020)	https://numpy.org/
	Pandas	Data frames and operations	Mckinney (2011)	https://pandas.pydata.org/
	Matplotlib	Plotting	Hunter (2007)	https://matplotlib.org/
	SciPy	Scientific computing	Virtanen et al. (2020)	https://github.com/scipy/scipy
	tqdm	Progress bar	Da Costa-Luis (2019)	https://github.com/tqdm/tqdm
Geospatial data processing	GeoPandas	Geospatial data processing and geometric operations	Jordahl et al. (2020)	https://geopandas.org/
	netCDF4	Processing NetCDF format data	Rew and Davis (1990)	https://github.com/Unidata/netcdf4-python
	Xarray	Processing multidimensional arrays and NetCDF format data	Hoyer and Hamman (2017)	https://github.com/pydata/xarray
	Rasterio	Processing gridded raster datasets	Gillies (2013)	https://github.com/rasterio/rasterio
	Cartopy	Spatial plotting and spatial reference	Office (2010-2015)	https://github.com/SciTools/cartopy
	Whitebox-Workflows	Hydrological analysis	Lindsay and Wu (2021)	https://www.whiteboxgeo.com/whitebox-workflows-for-python/
Optimization	DEAP	Evolutionary computation framework	Fortin et al. (2012)	https://github.com/deap/deap

3 Functionalities of the EVB

To make this study self-contained and easy to follow, basic descriptions, where necessary, of the functionalities of the EVB are provided in this section. Prior to describing the workflow of VIC deployment in the EVB, it is important to first introduce two related techniques.

3.1 Multiscale Parameter Regionalization technique

The Multiscale Parameter Regionalization (MPR) technique was pioneered by Samaniego et al. (2010), with the aim of proposing a method for the parameter estimation of distributed hydrological models at multiple scales. A distinctive feature of MPR is the combination of the transfer function and scaling operator. Following the information level division approach described earlier, at level 0, basin characteristics such as soil properties are transferred into effective parameters via the transfer function, after which the scaling operator is applied to scale these parameters to level 1. During this process, a set of spatially invariant, quasi-scale independent, scalar global parameters is used (hereafter referred to as g-parameters), making calibration possible and enhancing its applicability.

https://doi.org/10.5194/egusphere-2026-4655
Preprint. Discussion started: 12 August 2026

Notably, the feasible ranges of the g-parameters are constrained based on previous transfer-function studies, ensuring physically meaningful parameter bounds rather than arbitrary assignments. For example, according to the work of Cosby et al. (1984), the relationship between saturated hydraulic conductivity (K_S) and soil texture can be expressed as follows:

$$logK_s = 0.0126x - 0.0064y - 0.6, \tag{1}$$

where x denotes the sand content and y denotes the clay content. Using this empirical relationship as prior knowledge, a transfer function incorporating the g-parameters can be established, allowing K_S to be inferred from soil texture:

$$K_s = 10^{g_1+g_2x+g_3y}, \tag{2}$$

where g represents the g-parameters, and their feasible ranges (Table A1) can be obtained by proportionally scaling the coefficients from the original equation.

The MPR technique has been successfully applied to parameter estimation in various distribution hydrological models, including but not limited to the VIC and mHM models (Rakovec et al., 2016; Zink et al., 2017). All these studies have consistently demonstrated that the parameters estimated by MPR exhibit a certain degree of transferability. A recent study by Mizukami et al. (2017) is an important starting point for this study. They implemented the MPR technique for the VIC model using Fortran and generated parameter estimates for a large sample of basins across the CONUS. The EVB framework proposed here partially builds upon the transfer functions they used, with one improvement being its implementation in Python and in a modular, object-oriented manner rather than the original Fortran functional programming approach.

Additionally, we extended the MPR approach to include routing-module parameters. Specifically, the flow velocity and diffusion coefficient were regionalized based on grid-level river network information using mapping relationships reported in previous studies (Chen et al., 2019; Yang et al., 2016), resulting in spatially distributed parameter fields as formulated below:

$$v = g_1 \cdot acc^{g2} \cdot S^{g3}, \tag{3}$$

$$D = g_4 \cdot d \cdot v, \tag{4}$$

where acc is the accumulated upstream area, and S denotes the mean slope angle, d is the flow distance within each grid.

Within the EVB framework, the MPR method serves as a core module for VIC parameter estimation during the model deployment process. It offers the following advantages: (1) a user-friendly parameter estimation approach, with all parameter-related knowledge aggregated within the transfer function; (2) some extent of parameter transferability across

https://doi.org/10.5194/egusphere-2026-4655
Preprint. Discussion started: 12 August 2026

scales and regions; and (3) the consideration of the influence of basin characteristics on parameters, making them more physically meaningful.

3.2 General Unit Hydrograph technique

The Unit Hydrograph (UH) concept is a classical concept in hydrology, first introduced by Sherman (1932). Fundamentally, the rainfall–streamflow transformation is represented using a convolution-based transfer function model (TFM). Owing to its simple structure and computational efficiency, it can serve as an effective black-box routing approach. The RVIC routing model integrated within the VIC source code is a variant of the UH (Lohmann et al., 1996), which requires a grid UH for its parameter derivation.

Over the past decades, various forms of UH have been developed, such as the Nash UH based on a two-parameter Gamma distribution and the Soil Conservation Service (SCS) dimensionless UH. Among these forms, a General UH (GUH) introduced by Guo (2022a) has a particular appeal as it has explicit analytical expressions:

$$u(t) = \frac{dg}{dt} = \frac{\mu}{t_p} x(1 + mx)^{-(1+1/m)}, \tag{5}$$

$$g(t) = 1 - (1 + mx)^{-1/m}, \tag{6}$$

$$x(t) = exp\,[(\mu(\frac{t}{t_p} - 1))], \tag{7}$$

where t_p is the peak flow time; m is a dimensionless recessing coefficient determined by downstream water surface conditions; and μ is the rising coefficient related to the basin characteristics. This analytical expression provides high flexibility to the GUH and has been demonstrated to exhibit high consistency with traditional methods (Guo, 2022a). In this study, the GUH is employed as the default grid UH to derive the RVIC parameters. Its shape is controlled by the above three parameters, which are treated as free parameters to be calibrated. To enhance flexibility and user configurability, the Nash UH is also implemented as an optional alternative.

3.3 Workflow for VIC model deployment

Figure 1b presents the VIC model deployment workflow within the EVB framework, which consist of seven sequential steps. This deployment process follows the guidelines outlined in the official VIC documentation (https://vic.readthedocs.io/) and focuses on the image driver version of VIC-5. The following sections describe each workflow step to provide a concise overview of the deployment procedure.

https://doi.org/10.5194/egusphere-2026-4655
Preprint. Discussion started: 12 August 2026

3.3.1 Building of dpc instances

Based on data availability, format, and the discretization strategy required by the modelling objectives, users can construct instances of Grids and Basins classes and feed them into appropriate dpc instances for data processing. The processing pipeline is encapsulated within the data source-specific extractData_func, and computational efficiency can be improved through parallelization. Once the necessary data processing is completed, all derived information at both the basin and grid scales is persistently stored as instance attributes, facilitating static access for downstream deployment stages.

3.3.2 Building of domain file

A utility script, build_Domain, is designed to seamlessly accept a generated dpc instance at level 1 scale and construct the domain file required by VIC model in NetCDF format. This stage also includes the calculation of the area of each grid, its relative proportion within the basin, and the edge lengths in the latitudinal and longitudinal directions.

3.3.3 Building of VIC parameter files

Building VIC parameter files is a challenging task, as it involves accounting for both the physical interpretability of the parameters and their spatial variability across the modelling domain. Furthermore, several parameters like b_{infilt} and W_S lack clear physical meaning (Gou et al., 2020). For these parameters, calibration against the observed streamflow at the outlet is a standard procedure, but their spatial variability across grids significantly increases the dimensionality of the optimization search space, thereby prolonging the computation time.

To provide a user-friendly, efficient, and multiscale applicable VIC parameter preparation scheme, the EVB framework employs the MPR technique to build the parameter file, as described before. By design, the scheme can seamlessly accept a level 0 dpc instance as input and automatically generate the corresponding parameter file at desired modelling scale, while allowing the g-parameters to be calibrated according to specific calibration requirements.

3.3.4 Building of dpc instances

According to the guidelines in the official VIC-5 documentation, the minimum variable requirements for meteorological forcing include the following seven variables: average air temperature (AIR_TEMP), total precipitation (PREC), atmospheric pressure (PRESSURE), incoming shortwave radiation (SWDOWN), incoming longwave radiation (LWDOWN), vapor pressure (VP), and wind speed (WIND). For a typical meteorological forcing dataset, such as NLDAS2 (Xia et al., 2012), the VP is generally not included, whereas WIND is provided as two components: zonal and meridional wind speed (UGRD and VGRD). Therefore, the following formulas were used for conversion (Ahrens, 2015):

$$VP = \frac{SH \times PRESSURE}{0.622 + SH}, \tag{8}$$

https://doi.org/10.5194/egusphere-2026-4655
Preprint. Discussion started: 12 August 2026

$$WIND = \sqrt{UGRD^2 + VGRD^2}, \tag{9}$$

where *SH* is the specific humidity in kg/kg, and 0.622 is the gas constant ratio for dry air and water vapor. Adopting a similar architectural design, the buildMeteForcing function initiates processing from a dpc instance and follows a sequential workflow to generate multiple forcing data files in the NetCDF format. Although the initial processing may require some computational time, this procedure only needs to be performed once.

3.3.5 Building of RVIC parameter files

The RVIC is the official routing model of the VIC, grounded in the principle of the pulse response function between the source and sink. It convolves the runoff from the source grid cell produced by VIC, thereby generating streamflow at the outlet. Currently, the Python version of RVIC has been developed by the Computational Hydrology Group at the University of Washington (UW Hydro), encapsulated into a unified Python package (i.e., rvic), and organized into two components: parameter generation and routing. To fully leverage this, the current EVB framework uses the rvic Python package to generate the required parameter files, which are then passed to the VIC-RVIC coupling model for simultaneous runoff generation and routing. In the following, we present a detailed explanation of the RVIC parameter generation process.

First, a hydrological analysis based on the Digital Elevation Model (DEM) at the level 1 scale is performed to construct the hydrological topology. The EVB offers an implementation based on the Whitebox-Workflows Python package to generate a NetCDF file containing information about flow direction, source area, and flow distance. Then, a pour point file is generated according to the outlet coordinates specified by the user. Next, the UHBOX file, which contains a grid UH for a given time interval, needs to be provided by users based on prior knowledge. Here, we implement two alternative UHs in the create_uh module can be used: Nash UH and GUH. Finally, users need to create a configuration file based on the provided reference file. This configuration file controls the RVIC parameter generation process and includes two parameters—velocity and diffusion—which need to be determined by the users. There is a regionalization approach for the two parameters in the MPR framework, incorporating four g-parameters that require calibration, as detailed in Section 3.1. Overall, this stage generates a set of RVIC parameters for use within the VIC-RVIC coupling model.

3.3.6 Building of global parameter file

The global parameter file is a text file used to configure the VIC model, specifying input and output paths as well as runtime options. For convenience, a default global parameter file is provided as a reference, and a parsing module named GlobalParamParser is developed to facilitate reading, writing, and modifying the settings of this file. It allows the global parameter file to be read section by section and stored as an instance of a class.

https://doi.org/10.5194/egusphere-2026-4655
Preprint. Discussion started: 12 August 2026

3.3.7 Calibration of VIC model

Although the MPR technique embedded in the EVB framework is capable of directly estimating the spatially distributed parameters based on basin characteristics, a certain degree of calibration remains indispensable. This necessity arises from two primary sources of uncertainty. First, some parameters, such as the g-parameters in MPR and the two RVIC parameters (i.e., flow velocity and diffusion coefficient), cannot be fully determined through regionalization and therefore require calibration. Second, the scaling of these effective parameters from level 0 to level 1 may introduce additional uncertainties, potentially degrading the simulation performance of the VIC model (Todini, 2011). To address these issues, a parameter calibration module has been integrated into the EVB framework, enhancing the applicability of the VIC model across a broader range of basins.

The EVB framework implements two optimization algorithms for parameter calibration: the Covariance Matrix Adaptation Evolution Strategy (CMA-ES; Hansen and Ostermeier, 2001) for single-objective calibration and the Non-dominated Sorting Genetic Algorithm II (NSGA-II; Deb et al., 2002) for multi-objective calibration. Both algorithms are implemented using the DEAP Python library. CMA-ES provides an efficient strategy for single-objective optimization, whereas NSGA-II is capable of handling multiple objectives through its non-dominated sorting and crowding distance mechanisms. This implementation enables flexible calibration strategies, allowing users to incorporate additional observations beyond streamflow for multi-objective calibration, consistent with recent developments in hydrological model calibration (Széles et al., 2020; Mei et al., 2023).

4 Case basins and data collection

To illustrate the efficacy of the EVB framework in facilitating the flexible deployment of the VIC model, we designed two basin setups, each representing a typical research scenario. The former exemplifies the increasingly popular large-sample basin research paradigm (Yeste et al., 2024), whereas the latter corresponds to the more traditional site-specific approach in hydrological studies. Then, these two basin setups were used as test cases to assess the performance and efficiency of the EVB-VIC modelling framework across multiple hydrological applications. The subsequent section delineates the basin setups and the requisite data for model implementation.

4.1 Basin setup A: case basin from large-sample dataset

Throughout the history of hydrological modelling research, there has been an ongoing debate between the paradigms of depth and breadth. Gupta et al. (2014) argued the past hydrological practice tended to emphasize depth over breadth, with model development and process studies often confined to individual or a limited number of basins. Drawing on the analogy of crash testing, Andréassian et al. (2009) highlighted that both research approaches—site-specific and large-sample studies—are essential. Such appeals have led to the development of influential large-sample datasets, including Terrestrial

https://doi.org/10.5194/egusphere-2026-4655
Preprint. Discussion started: 12 August 2026

Environmental Observatories (TERENO; Zacharias et al., 2011), Model Parameter Estimation Experiment (MOPEX; Duan et al., 2005), and Catchment Attributes and Meteorology for Large-sample Studies (CAMELS; Newman et al., 2015; Addor et al., 2017), which have further facilitated the application of large-sample hydrological research. Therefore, giving these emerging research needs, it is meaningful to explore the potential of the EVB framework to be seamlessly applied to large-sample dataset for VIC modelling.

In this study, we selected a case basin from CAMELS dataset to demonstrate the implementation of VIC modelling within the EVB framework. Employing a simple model setup with streamflow-only calibration, we investigated the parameter transferability to evaluate the efficiency of applying EVB in large-sample basin contexts. The case basin is located within Missouri, USA, and is known as the Gasconade River Basin (GRB; USGS gauge ID: 06934000), with a total drainage area of approximately 8,268 km2. Fig. 2 provides an illustrative map of the basin, showcasing the topography, outlet, and land surface properties in the area. The local temperate continental climate is typical and characterized by distinct seasonal variations. Under the combined effects of climate, topography, and vegetation, streamflow in this area exhibits pronounced seasonal variability, with the peak flow occurring in the spring and a low flow observed in the late summer and autumn. Notably, the current EVB implementation, once demonstrated in this case basin, can be seamlessly extended to the entire CAMELS basin collection.

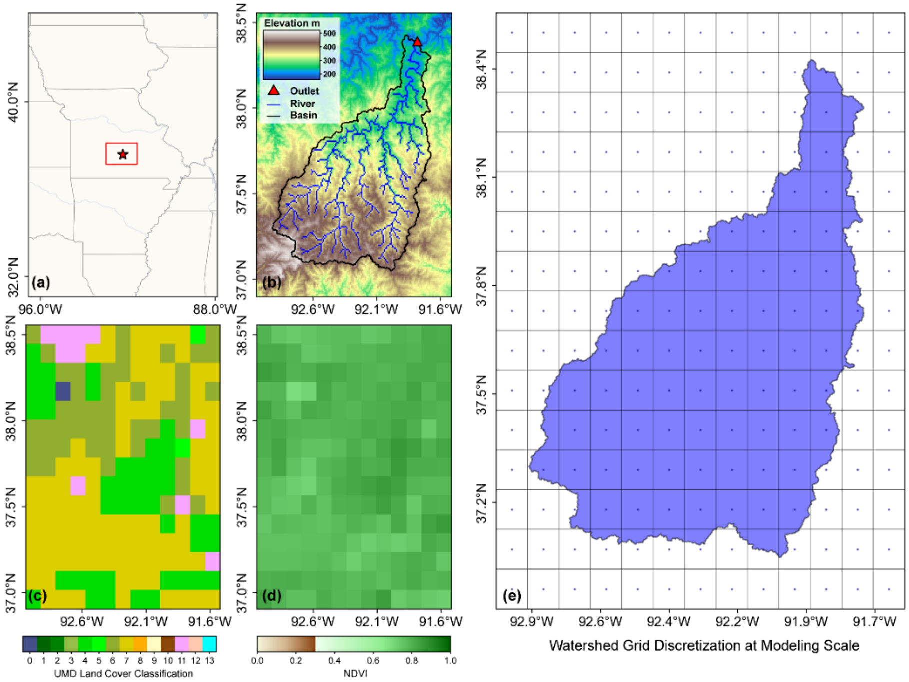

Figure 2. Overview of the Gasconade River Basin. (a) Location within Missouri, USA. (b) Topography, river network, and outlet location. (c) Dominant land cover classes according to the University of Maryland Global Land Cover dataset (Hansen et al., 2021). (d) Averaged NDVI from the MOD13A3.061 dataset (Didan, 2021). (e) Watershed grid discretization at modelling scale (i.e., 12 km × 12 km).

https://doi.org/10.5194/egusphere-2026-4655
Preprint. Discussion started: 12 August 2026

4.2 Basin setup B: single site-specific basin

Beyond large-sample applications, we further assess the adaptability of the EVB to the single site-specific basin setup, a typical case in which researchers define or customize their own study domain. Within this setup, a more complex multi-objective calibration was employed, alongside an in-depth examination of the physical plausibility of the spatial parameter distributions. Here, we selected the Jing River Basin (hereafter referred to as JRB), with a drainage area of approximately 45,400 km2, as the case basin. It represents a markedly different hydroclimatic setting compared to GRB, characterized by a typical arid to semi-arid climate and land use condition representative of northern China (Fig. 3).

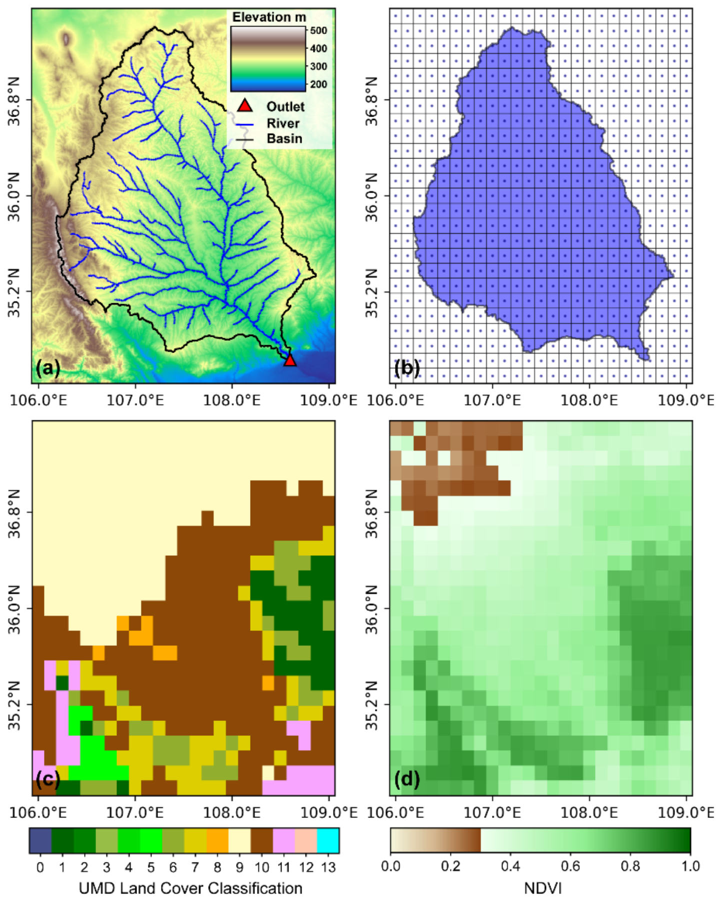

Figure 3. Overview of the Jing River Basin. (a) Topography, river network, and outlet location. (b) Watershed grid discretization at modelling scale (i.e., 13.8 km × 13.8 km). (c) Dominant land cover classes according to the University of Maryland Global Land Cover dataset (Hansen et al., 2021). (d) Averaged NDVI from the MOD13A3.061 dataset (Didan, 2021).

https://doi.org/10.5194/egusphere-2026-4655
Preprint. Discussion started: 12 August 2026

4.3 Data collection

4.3.1 Datasets used in basin setup A

The extracted information on daily streamflow, basin boundaries, and outlet location of GRB from the CAMELS dataset provides essential input for deploying the VIC model. Other distributed data are also required. First, the hourly forcing, including precipitation, downward longwave radiation, downward shortwave radiation, surface pressure, specific humidity, air temperature, and wind speed, was acquired from Phase 2 of the North American Land Data Assimilation System (NLDAS-2) forcing dataset with a spatial resolution of 0.125° and covering the period from 1998 to 2010 (Xia et al., 2012). This dataset was originally developed to force several LSMs, including VIC, and it is derived from the analysis fields of NCEP North American Regional Reanalysis (NARR). It has been validated in a range of hydrological modelling studies, demonstrating robust applicability (Sun et al., 2021; Yan et al., 2023).

Second, several datasets were collected to describe the static features of the underlying surface (i.e., soil, topography, land cover type, and vegetation). Specifically, the soil texture (i.e., the proportions of sand, loam, and clay) and the bulk density of 11 soil layers (ranging from 0 to 2.5 m in depth) were obtained from the conterminous United States (CONUS-SOIL) dataset (Miller and White, 1998). The data from the Shuttle Radar Topography Mission (SRTM) Digital Elevation Model (DEM) V4.1 (90 m) were used to describe the topography (Jarvis et al., 2008). The 1 km gridded global land cover dataset from the University of Maryland (UMD Land Cover) provides information on 14 land cover classes (Hansen et al., 2021). Vegetation information includes monthly data on the partial vegetation cover fraction (fcanopy), the leaf area index (LAI), and the albedo. Following previous studies, the fcanopy can be derived from the Normalized Difference Vegetation Index (NDVI) using the following formula (Bohn and Vivoni, 2019):

$$f_{canopy} = \left(\frac{NDVI - NDVI_{min}}{NDVI_{max} - NDVI_{min}}\right)^2, \tag{10}$$

On this basis, multi-year data for albedo, NDVI, and LAI were extracted from several derived Moderate Resolution Imaging Spectroradiometer (MODIS) products (MCD43D51.061, MOD13A3.061, and MOD15A2H.061) and mosaicked into monthly values. Finally, the four-layer soil temperature from the ERA5 Land product is extracted and averaged to serve as the bottom boundary condition for the soil heat flux in the VIC model.

4.3.2 Datasets used in basin setup B

For site-specific VIC modelling application, we incorporated additional datasets applicable to the JRB, alongside the aforementioned global datasets. These include SoilGrids1km for detailed soil property information (Hengl et al., 2014; Poggio et al., 2021) and the China Meteorological Forcing Dataset (CMFD) for localized meteorological forcing (He et al.,

https://doi.org/10.5194/egusphere-2026-4655
Preprint. Discussion started: 12 August 2026

2020). The latter provides high spatiotemporal resolution (0.1°, 3 hourly) data for seven essential variables across China, making it well-suited for constructing meteorological forcing inputs required by the VIC hydrological model in JRB.

As mentioned above, we considered different complementary objectives during the calibration process. On the one hand, we evaluated the model's ability to reproduce the temporal dynamics of streamflow by comparing the simulated results with in situ observations from the Zhangjiashan hydrological station (108.60°E, 34.63°N; Fig. 3a). On the other hand, we assessed its capability to capture the patterns of actual evaporation and soil moisture. The reference data of these two variables were obtained from the Global Land Evaporation Amsterdam Model (GLEAM) dataset (Martens et al., 2017). Since the GLEAM dataset employs a conceptual water balance soil module, the surface (0-10 cm) and root-zone (10-100 cm) soil moisture were aggregated to estimate total soil moisture, so as to allow a comparison with the VIC model outputs. In this context, analyzing the patterns consistency between the simulated and reference data proves more meaningful than direct magnitude comparisons.

The datasets listed above are publicly available and widely used in hydrological modelling. An overview of these datasets is provided in Table 2.

Table 2. An overview of the datasets used for deploying the VIC model.

Datasets	Description	Resolution	Reference
CAMELS	Large-sample basin datasets providing streamflow observations and basin boundaries	Basin scale	Newman et al. (2015); Addor et al. (2017)
GLEAM	Actual evaporation and soil moisture dataset	0.25° × 0.25°	Martens et al. (2017)
NLDAS-2	Meteorological forcing dataset	0.125° × 0.125°	Xia et al. (2012)
CMFD	Meteorological forcing dataset	0.1° × 0.1°	He et al. (2020)
CONUS-SOIL	Soil properties dataset	30'' × 30''	Miller and White (1998)
SoilGrids1km	Soil properties dataset	1 km × 1 km	Hengl et al. (2014); Poggio et al. (2021)
SRTM DEM	Digital elevation dataset	90 m × 90 m	Jarvis et al. (2008)
UMD Land Cover	Land cover dataset	1 km × 1 km	Hansen et al. (2021)
MCD43D51.061 BSA	MODIS black sky albedo dataset	1 km × 1 km	Schaaf and Wang (2021)
MOD13A3.061 NDVI	MODIS NDVI dataset	1 km × 1 km	Didan (2021)
MOD15A2H.061 LAI	MODIS LAI dataset	500 m × 500 m	Myneni et al. (2021)
ERA5 Land ST	ERA5 Land soil temperature dataset for four layers	0.1° × 0.1°	Muñoz Sabater (2019)

https://doi.org/10.5194/egusphere-2026-4655
Preprint. Discussion started: 12 August 2026

5 Modelling Applications based on the EVB

5.1 VIC Model deployment

The VIC model instances were deployed via the EVB framework at multiple spatial resolutions (i.e., 6, 8, and 12 km) in basin setup A, and at a fixed resolution (i.e., 13.8 km) in basin setup B. The spatial resolutions of level 0 and level 2 are determined based on the data availability and are set to 1 km and 0.125°, respectively. The data listed in Table 2 were resampled to the corresponding spatial resolutions, and the input files required for running VIC were generated following the deployment workflow described above.

To provide a full narrative of the VIC deployment, there are two configurations that need to be clarified—data partitioning and parameter calibration. For basin setup A, the period from 1998 to 1999 served as a warm-up period to ensure stable initial conditions. The model was then calibrated using daily streamflow records from 2000 to 2007 to derive the optimal parameter set, with the remaining 3 years reserved for validation. For the objective function, we use the KGE metric on streamflow, which is a widely recognized measure of model performance that integrates bias, variance, and correlation (Gupta et al., 2009). Further evaluation metrics, including NSE and PBIAS, are employed to comprehensively evaluate model performance during the validation period (Mizukami et al., 2019). Formally, these metrics can be calculated using the following formulas:

$$KGE = 1 - \sqrt{(r-1)^2 + (\frac{\sigma_{sim}}{\sigma_{obs}} - 1)^2 + (\frac{\mu_{sim}}{\mu_{obs}} - 1)^2}, \quad (11)$$

$$NSE = 1 - \frac{\sum_{i=1}^{n}(V_{obs}^{i} - V_{sim}^{i})^2}{\sum_{i=1}^{n}(V_{obs}^{i} - \overline{V}_{obs})^2}, \quad (12)$$

$$PBIAS = \frac{\sum_{i=1}^{n}(V_{obs}^{i} - V_{sim}^{i})}{\sum_{i=1}^{n} V_{obs}^{i}} \times 100\%, \quad (13)$$

where σ is the standard deviation; and μ is the mean; V^i is the target variable (i.e., streamflow) at time step i; and n is the length of the sequence. The subscripts *sim* and *obs* denote the simulated and observed values. Both KGE and NSE are formulated such that higher values indicate better model performance, with a value of 1 representing the optimal simulation for each metric. The final metric, PBIAS, is used to evaluate whether the model overestimates (PBIAS < 0) or underestimates (PBIAS > 0) the observed values.

In the case of basin setup B, the years 2008–2009 were allocated for model warm-up, 2010-2015 for calibration, and 2016-2018 for validation. A special setting in this setup is that multiple objective functions were formulated to improve the simulation performance with respect to various aspects of the VIC model during the calibration process. Besides using KGE

https://doi.org/10.5194/egusphere-2026-4655
Preprint. Discussion started: 12 August 2026

to evaluate streamflow and actual evaporation simulation, the model capability to reproduce the patterns of soil moisture was assessed via the Pearson correlation coefficient (R), which is formulated as follows (Wambura et al., 2018):

$$R = \frac{\sum_{i=1}^{n}(V_{obs}^{i}-\overline{V_{obs}})(V_{sim}^{i}-\overline{V_{sim}})}{\sqrt{\sum_{i=1}^{n}(V_{obs}^{i}-\overline{V_{obs}})^2}\sqrt{\sum_{i=1}^{n}(V_{sim}^{i}-\overline{V_{sim}})^2}}, \tag{14}$$

where V^i is the target variable at time step i and the overbar indicates the average.

In this study, parameter calibration was performed using the CMA-ES and NSGA-II algorithm implemented in the EVB, as described in Section 3.3.7. The CMA-ES algorithm is configured with a population size of 40, and the initial global step size (σ) is set to 0.4. The NSGA-II algorithm is configured with a population size of 20, a crossover probability of 0.7, and a mutation probability of 0.2. Polynomial mutation and simulated crossover are employed. To mitigate potential identifiability issues arising from a large number of free parameters, we fixed some of the physical parameters and introduced a simplified calibration set, reducing the free parameters from 44 to 15. According to previous studies (Cortés-Salazar et al., 2023; Yeste et al., 2024), this minimal parameter set is considered to contain only the sensitive parameters. All 15 free parameters (Table A2) are treated equivalently within a parameter pool and sampled by Latin hypercube sampling (LHS) to partition the parameter space into equiprobable regions with representative samples, thereby ensuring efficient coverage of entire parameter range (McKay et al., 1979).

The optimization was performed for a maximum of 200 generations and stopped upon convergence, with the optimal parameters selected according to the maximum KGE in basin setup A. For the multi-objective calibration in basin setup B, a best Pareto front comprising multiple non-dominated optimal solutions was generated, from which a solution exhibiting a relatively balanced trade-off among objectives was manually selected as the final parameter set. The convergence process of the single-objective calibration and the Pareto front curves from the multi-objective calibration are provided in Fig. B1 and B2, respectively.

Noteworthily, all experiments in this study were performed on a laptop with 32.0 GB of RAM, with an AMD Ryzen 7 8845H 3.80 GHz processor, and running Ubuntu 20.04.1 LTS (virtual machine). To illustrate the computational efficiency of EVB, the average time required for each step of the deployment process in the second case application, as described later, was recorded, as shown in Table 3. Building dpc instances and processing meteorological forcing data are the primary time-consuming steps, but both need to be executed only once per modelling application and can thereafter be saved to persistent storage for convenient reuse. Additionally, the time consumption of these steps is influenced by the modelling scale and data sources, and thus may vary across different applications.

https://doi.org/10.5194/egusphere-2026-4655
Preprint. Discussion started: 12 August 2026

Table 3. Time consumption for EVB deployment workflow.

Step No.	Deployment Step	Description	Time Spent (seconds)
1	Build dpc instances	Initialize data processing classes for handling input data	13,200
2	Build domain file	Generate domain file	38
3	Build VIC parameter files	Generate parameter files at level 0 and level 1 scales	20
4	Build meteorological forcing files	Process and format meteorological data inputs	9600
5	Build RVIC parameter files	Prepare parameter files required by the RVIC routing model	75
6	Build global parameter file	Generate global parameters to control the VIC model run	1
7	Run VIC-RVIC coupled model	Perform one run of the VIC-RVIC coupled model	32
8	Sample and regenerate parameter files	Perform one round of parameter sampling and regeneration during calibration	14

5.2 Modelling application in basin setup A

5.2.1 Parameter transferability across different spatial scales

Proceeding from the simplest case, we examined the capability of the coarsest-resolution (i.e., 12 km) VIC configuration to simulate daily streamflow. As shown in Fig. 4, the seasonal and event-based variations in streamflow are generally well reproduced, although some fluctuations remain in the simulated time series. The evaluation metrics also indicate a satisfactory performance, with KGE, NSE, and PBIAS values of 0.60, 0.61, and −28.67% for the calibration period. The corresponding values for the validation period (0.60, 0.63, and −5.92%) indicate no substantial degradation in performance. We further evaluated model performance separately for low-flow (< 30th percentile) and high-flow (> 70th percentile) regimes, defined based on the total streamflow range. In this way, a consistent pattern in model behaviour emerged across different periods, dominated by a pronounced overestimation during low-flow conditions and a slight underestimation during high-flow conditions (right panels in Fig. 4). Such behaviour was also appreciated in the detailed analyses of previous studies (Wenger et al., 2010; Lehmann et al., 2022). Overall, the above analysis indicates that the streamflow simulation performance is acceptable.

We next evaluate the transferability of parameters across spatial scales—a key feature of EVB's deployment potential to support VIC applications under different spatial configurations. To this end, the 15-parameter set calibrated at 12 km resolution was transferred to 6 km and 8 km models (hereafter denoted as VIC-6, VIC-8, and VIC-12). The resulting simulations were then compared to access parameter transferability. Fig. 5 provides an intuitive comparison of model performance in streamflow simulation through Taylor diagram analysis. Both panels of the figure suggest that parameters transfer from a coarser resolution (12 km) to finer resolutions (6km and 8 km) preserves model performance, as evidenced by the close clustering of three points in Taylor diagram space. Figs. C1 and C2 present the simulated hydrographs and corresponding evaluation metrics for the VIC-8 and VIC-6 models. Although calibration-period performance of transferred

https://doi.org/10.5194/egusphere-2026-4655
Preprint. Discussion started: 12 August 2026

models declined relative to VIC-12, it remained within acceptable thresholds (KGE > 0.50, NSE > 0.58). Importantly, no degradation occurred during the validation period, with both KGE and NSE of transferred models exceeding 0.62. Such parameter transferability was achieved through the MPR technique, which links different spatial scales using the same underlying input data at level 0 and the corresponding transferred g-parameters.

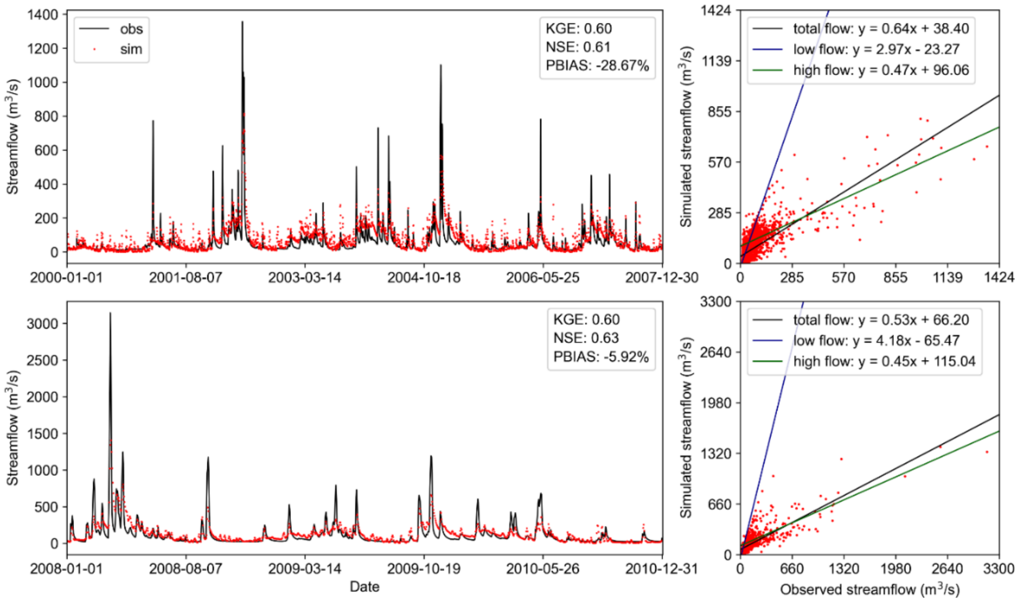

Figure 4. Comparison of daily simulated streamflow from the 12 km-resolution VIC model against observations during the calibration period (top two panels) and validation period (bottom two panel). Low-flow and high-flow thresholds are defined as 30th and 70th percentiles of the total flow range, respectively.

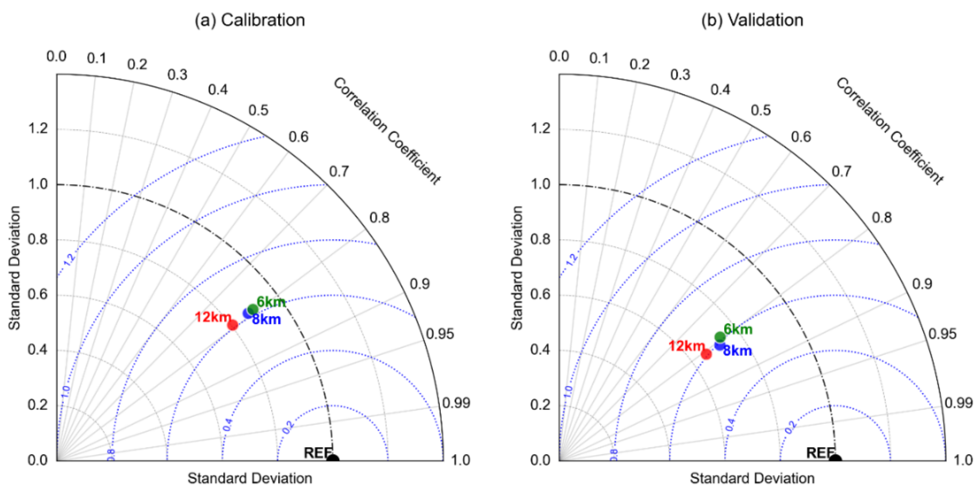

Figure 5. Taylor diagrams of daily simulated streamflow from the VIC model at three spatial scales (6 km, 8 km, and 12 km). Both simulated and observed values are standardized, with the observed values (REF point) having a standard deviation of 1.0. Blue dashed contours indicate root mean square error (RMSE) relative to observed benchmarks.

https://doi.org/10.5194/egusphere-2026-4655
Preprint. Discussion started: 12 August 2026

5.2.2 Distributed simulations of surface runoff and baseflow

Surface runoff and baseflow are recognized as the dominant hydrological components governing high-flow and low-flow conditions, respectively, and are often conceptualized as rapid response and slow response processes within watershed systems (Liu et al., 2012a; Singh et al., 2018). From this perspective, the analysis presented in the preceding section raised a critical question: given that the model has demonstrated scale transferability in hydrograph simulation, does it also reproduce consistent spatial distributions of runoff generation processes across different scales? To address this issue, we selected a representative single-peak flood event spanning the period of February 1, 2001, to March 31, 2001, to examine the runoff generation processes across varying scales. Specifically, we focus on the distributed simulations of particular components—namely, the surface runoff during the rising period and the baseflow during the recession period.

The event-based simulation results are presented in Fig. 6, showcasing the streamflow hydrographs alongside the spatial distribution of the two runoff components. A clear observation is that the three simulated hydrographs exhibit remarkable consistency. The spatial distribution of surface runoff during the rising phase illustrates the runoff generation processes, peaking on February 24, coinciding with the timing of the peak rainfall (Fig. 6b), while the routed flow took approximately two days to reach the hydrograph peak at the outlet (Fig. 6a). This pattern is consistent across resolutions without significant magnitude variations. In terms of the distributed simulation of baseflow, all models consistently produced only a minor decrease in the central part of the basin during the recession period. This indicates that the model interprets this flood event as primarily dominated by surface runoff, whereas baseflow maintaining the multi-year baseline discharge in the river channel. Another finding from Fig. 6 is the pronounced underestimation of peak flows, which our analysis suggests stems from inadequate surface runoff generation. This could potentially be improved in future calibrations by including peak-flow-focused signature metrics in the objective function (Mizukami et al., 2019).

https://doi.org/10.5194/egusphere-2026-4655
Preprint. Discussion started: 12 August 2026

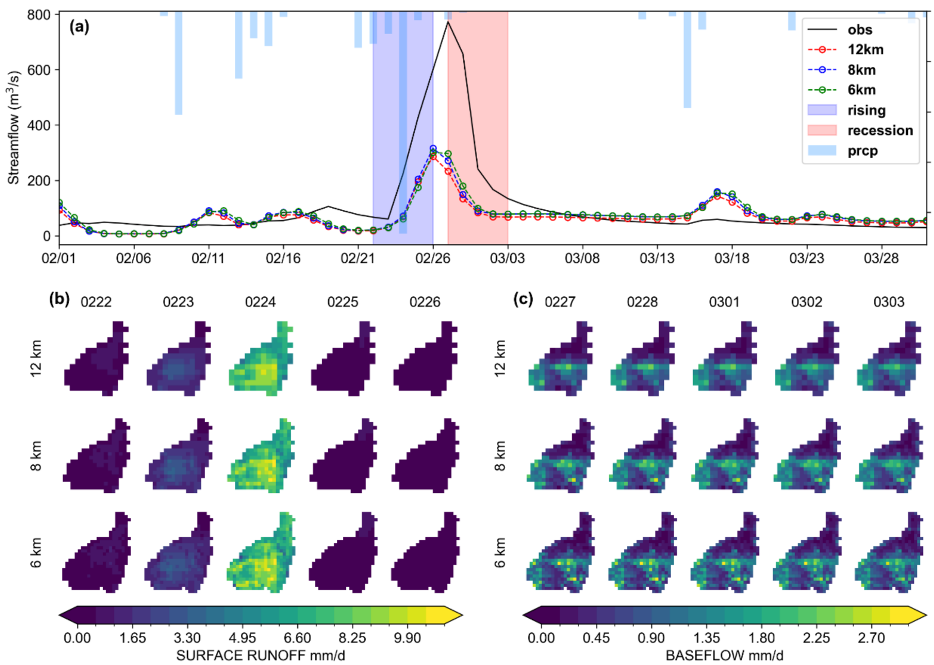

Figure 6. Scatterplots of daily simulated streamflow from the VIC model at three spatial scales (6 km, 8 km, and 12 km) against observations. The total sample is partitioned into low-flow and high-flow subsets for comparative evaluation, with the thresholds set at the 30th and 70th percentiles of the total flow range.

5.3 Modelling application in basin setup B

5.3.1 Multi-objective simulation performance

Relying solely on single-objective calibration using outlet streamflow is increasingly considered insufficient to address the growing demands of the hydrological modelling community (Beven., 2024). To support the goal of producing the right results for the right reasons and to improve model credibility, it is essential to integrate multiple data sources into the calibration process. In this section, we explore this potential application in the JRB basin.

Figure 7 shows the VIC simulation results obtained with the optimal parameter set derived from a three-objective calibration against streamflow, actual evaporation, and soil moisture. It can be seen that streamflow performance is acceptable in both the calibration and validation periods, with KGE exceeding 0.7 and absolute PBIAS below 3%, indicating good simulation of total streamflow. However, NSE values below 0.5 indicate that the VIC model performs relatively poorly in capturing peak flows in the JRB basin, as NSE is particularly sensitive to high flows (Mizukami et al., 2019; Zhong et al., 2023). Such behaviour has been documented in earlier VIC modelling studies, especially for arid basins similar to the JRB (Gou et al., 2020; Lehmann et al., 2022). In terms of evaporation, the VIC model reproduces the seasonal variation pattern well (KGE > 0.8), but it tends to overestimate certain summer peaks, as indicated by the red dots for May–August in this figure. As the

https://doi.org/10.5194/egusphere-2026-4655
Preprint. Discussion started: 12 August 2026

soil depth is adjusted during the calibration process, comparing the temporal correlation between simulated and GLEAM SM is more meaningful than compare absolute values at fixed depths, thus effectively avoiding the conceptual mismatch issue (Liu et al., 2012b; Chagas et al., 2024). The comparison of standardized SM values shown in the last row of Fig. 8 indicates good agreement between simulated and observed values (R > 0.85). Complementing the results presented above, our previous study (Zheng et al., 2026a) also demonstrated the capability of the EVB-deployed VIC model to support multi-objective applications through calibration against runoff observations from multiple gauging stations. Collectively, these findings indicate that the EVB framework provides a robust foundation for flexible and comprehensive hydrological simulations.

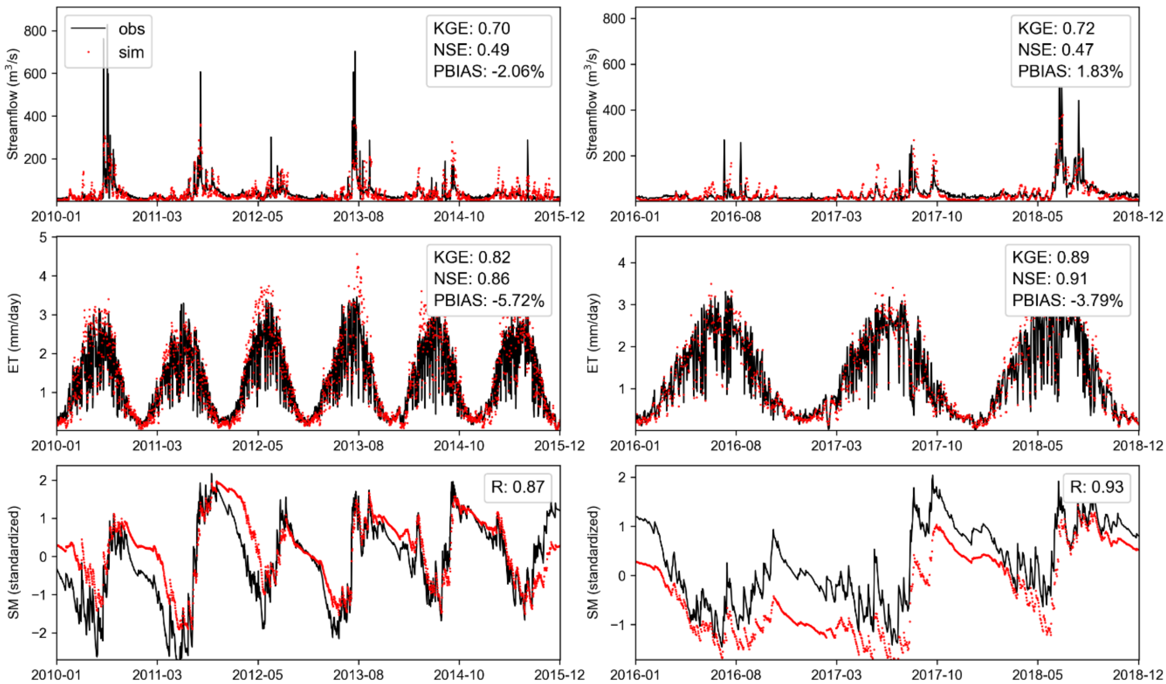

Figure. 7. Daily simulated versus observed values under three-objective calibration, including streamflow, actual evaporation (ET), and standardized soil moisture. The left panels represent the calibration period, and the right panels represent the validation period.

5.3.2 Physical plausibility of spatial parameter patterns

A central concern in hydrological modelling is the reliability of spatial parameters, which are estimated from MPR in this study. Interpreting key VIC parameters in physically meaningful term is essential for establishing model credibility and ensuring "right results for right reason". Here, we designed a synthetic single-peak rainfall event lasting two days with a total precipitation of 100 mm (Table 4), applied uniformly as the forcing input to the previously calibrated VIC model. The initial soil moisture was set to 70% of the basin-average field capacity (*FC*) for the upper two soil layers and 80% of *FC* for the

https://doi.org/10.5194/egusphere-2026-4655
Preprint. Discussion started: 12 August 2026

bottom layer, to ensure consistent initial conditions across all grid cells. In this experiment, spatial variability arises solely from the model parameters, and thus their physical plausibility can be verified through the relationship between simulation results and spatial parameter patterns.

Table 4. Meteorological conditions of the synthetic single-peak rainfall event.

Time	PRE (mm)	TMP (°C)	WIND (m/s)	LWD (W/m^2)	SWD (W/m^2)	VP (kPa)	PRS (kPa)
2025/1/1 0:00	0	20	3.0	300	600	1.0	101.0
2025/1/1 3:00	0	21	3.0	310	650	1.1	101.2
2025/1/1 6:00	5	20	2.5	305	500	1.2	101.1
2025/1/1 9:00	10	19	2.0	295	300	1.4	100.9
2025/1/1 12:00	20	18	1.5	290	200	1.6	100.7
2025/1/1 15:00	30	17	1.0	285	100	1.8	100.5
2025/1/1 18:00	20	18	1.5	290	200	1.6	100.7
2025/1/1 21:00	10	19	2.0	295	300	1.4	100.9
2025/1/2 0:00	5	20	2.5	300	500	1.3	101.0
2025/1/2 3:00	0	21	3.0	310	600	1.1	101.2
2025/1/2 6:00	0	21	3.0	310	600	1.0	101.3
2025/1/2 9:00	0	21	3.0	310	600	1.0	101.3
2025/1/2 12:00	0	22	3.0	315	650	1.0	101.4
2025/1/2 15:00	0	22	3.0	315	650	1.0	101.4
2025/1/2 18:00	0	22	3.0	315	650	1.0	101.4
2025/1/2 21:00	0	22	3.0	315	650	1.0	101.4

*Note: PRE, precipitation; TMP, air temperature; WIND, wind speed; LWD, downward longwave radiation; SWD, downward shortwave radiation; VP, vapor pressure; PRS, surface pressure.

We first examined the relationship between total surface runoff and the abstract variable infiltration curve parameter (b_{infilt}), which has been identified in previous studies as a highly sensitive parameter in the VIC model (Gou et al., 2020). As shown in Fig. 8, the the spatial distribution of slope is strongly reflected in the runoff map, with areas characterized by lower terrain slopes exhibiting reduced runoff generation, such as the central part of the basin, the northwestern and southeastern corner. This pattern is physically plausible, as flatter plain areas generally produce less runoff than steeper mountainous regions. From a computational perspective, this correspondence arises from the application of the MPR technique, in which slope is explicitly incorporated as an input for estimating the b_{infilt} at the level 0 scale (Fig. 8c). During the subsequent upscaling from the level 0 to the level 1, b_{infilt} governs the partitioning of rainfall between infiltration and surface runoff, with higher values reducing infiltration and enhancing surface runoff (Carvalho et al., 2022). Compared with spatially uniform parameters, the MPR-based estimates appear to be more physically plausible.

Next, we focus on the baseflow process. As presented in Fig. 9a, the influence of topography on runoff is also reflected in the total baseflow, with low values observed in the central basin. Moreover, a north–low to south–high gradient is apparent

https://doi.org/10.5194/egusphere-2026-4655
Preprint. Discussion started: 12 August 2026

around 36.375° N, which is in line with the runoff yield distribution previously simulated using the Water and Energy Transfer Processes (WEP) model (Zhang et al., 2023) and aligns with the regional north–south transition from semi-arid to semi-humid climatic conditions (Jia et al., 2015). Computationally, this behaviour is governed by W_S—the proportion at which nonlinear baseflow begins (Yeste et al., 2024). In the drier northern regions with weaker soil water retention, soil texture leads to lower field capacity (*FC*) values (Fig. 9c–f), which in turn result in larger estimated W_S values, thereby reducing baseflow generation (Fig. 9a-b). This spatial variability of W_S agrees with the expected role of soil water availability in controlling nonlinear baseflow activation, highlighting the physical interpretability of the calibrated parameter.

Finally, the plausibility of the estimated parameters was assessed through comparison with reference datasets from prior study. Specifically, two physically meaningful variables, field capacity (*FC*) and wilting point (*WP*) were evaluated against the Soil Hydraulic Parameters for China released by Dai et al. (2013), which has been widely adopted in hydrological and land surface modeling applications (Miao et al., 2020, Gou et al., 2021). The corresponding spatial distributions are shown in Fig. 10. Clearly, both *FC* and *WP* preserve the spatial patterns of the reference values after calibration, with a pronounced south-to-north decreasing gradient that reflects the higher soil water retention capacity in the southern JRB. In terms of magnitude, the calibrated *FC* values fall within nearly the same range as the reference values, while the *WP* values are slightly higher; considering differences in soil layer conceptualization and potential scale effects, these discrepancies are deemed acceptable.

In summary, the above results support the physical plausibility of the estimated parameters, as reflected in their consistency with runoff processes and reference dataset. Furthermore, the coherence between the underlying input data (soil properties and topography) and the highly abstract parameters underscores the rationality of MPR-based parameter estimation, which is facilitated by the use of transfer functions (Mizukami et al., 2017).

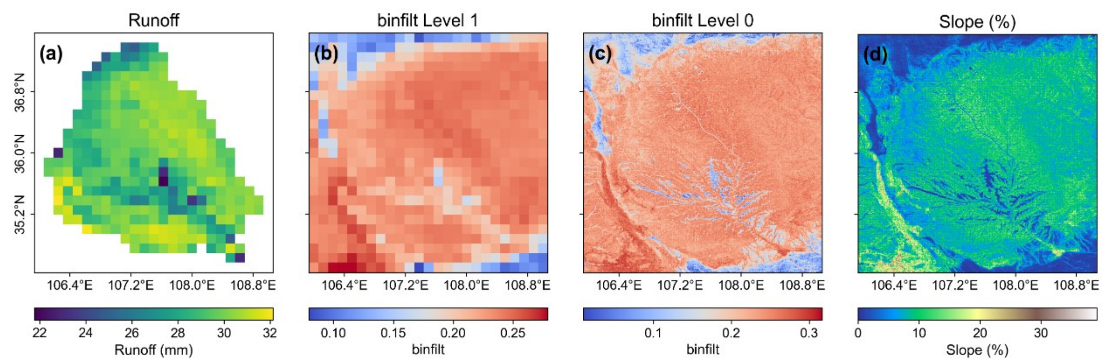

Figure. 8. Spatial distribution of (a) total surface runoff, (b) b_{infilt} parameter at level 1 scale, (c) b_{infilt} parameter at level 0 scale, and (d) terrain slope.

https://doi.org/10.5194/egusphere-2026-4655
Preprint. Discussion started: 12 August 2026

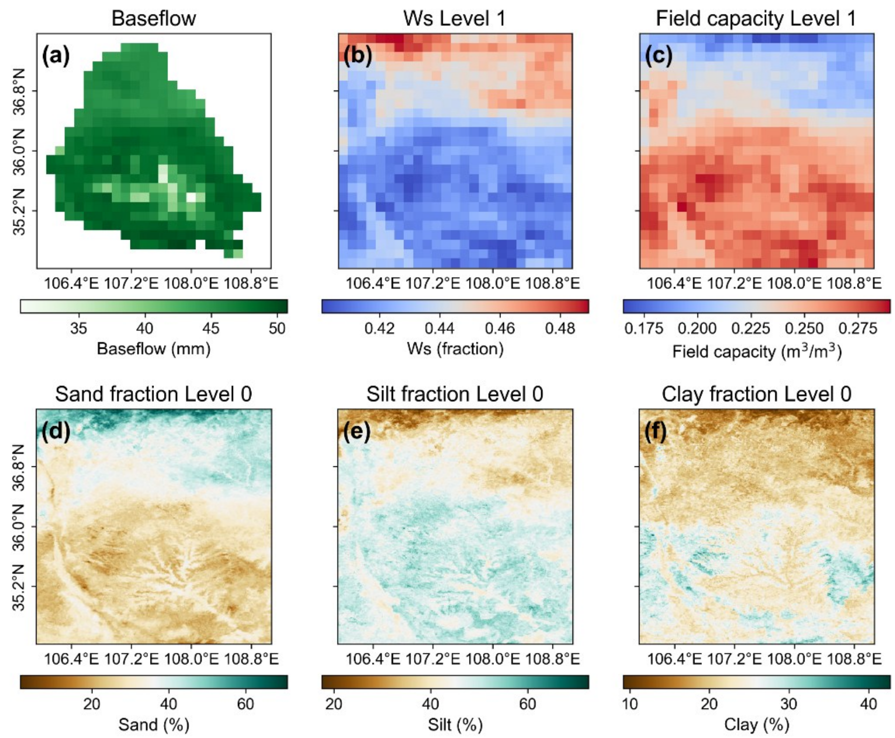

585 **Figure. 9. Spatial distribution of (a) total baseflow, (b) *Ws* parameter, (c) field capacity (*FC*), and (d–f) soil texture components: sand, silt, and clay fractions, respectively.**

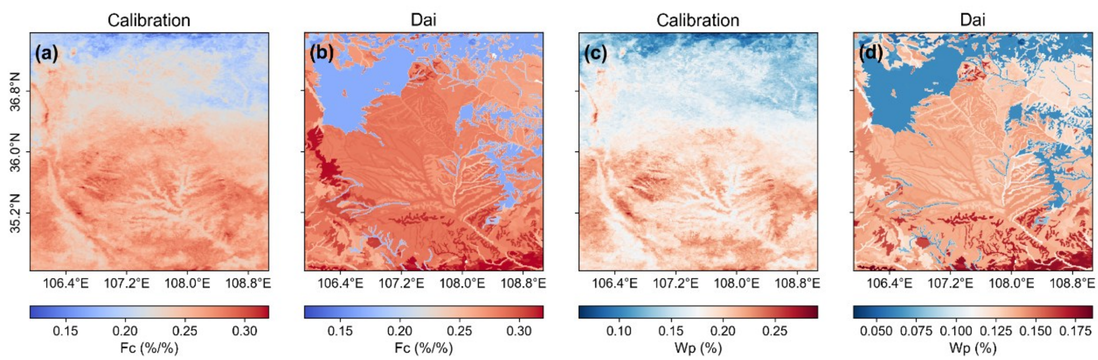

Figure. 10. Spatial distribution of field capacity (*FC*) and wilting point (*WP*). Panels (a, c) show parameters estimated through model calibration, while panels (b, d) are derived from Dai et al. (2013).

https://doi.org/10.5194/egusphere-2026-4655
Preprint. Discussion started: 12 August 2026

6 Conclusion

This study was motivated by the need for a standardized and reproducible approach to VIC model deployment. Although the restructuring of VIC-5 has enhanced its flexibility and maintainability, it has introduced additional technical complexity for model implementation. To overcome these limitations, we developed an open-source Python framework, Easy VIC Build (EVB), which provides a flexible and efficient solution for automated VIC model deployment.

The EVB framework adopts a modular object-oriented architecture and integrates advanced techniques for VIC model deployment, including the Multiscale Parameter Regionalization (MPR) and the General Unit Hydrograph (GUH). Through the implementation of several core classes—such as Grids and Basins for storing and processing geographic information, dpc for managing forcing and general input data, and Evb_dir for organizing file paths—together with a layered abstraction strategy based on information-level division, EVB enables efficient data management and seamless information transfer throughout the model deployment workflow.

The efficiency of the EVB framework was evaluated through several real-world modelling applications implemented across two distinct basin setups. The results demonstrate that EVB-VIC can generate spatially distributed parameters fields while maintaining robust parameter transferability across different spatial resolutions. Multi-objective calibration experiments and assessments of the physical consistency of spatial parameter patterns further support the reliability and credibility of the simulations. Overall, we anticipate that the EVB framework will facilitate broader applications of the VIC model by improving compatibility with VIC-5 and providing standardized, flexible, and efficient deployment capabilities beyond those offered by existing tools.

.

https://doi.org/10.5194/egusphere-2026-4655
Preprint. Discussion started: 12 August 2026

Appendix A Free parameters calibrated in the Easy VIC Build framework

Table A1. Full set of 44 free parameters for calibration (Guo, 2022a; Lohmann et al., 1996; Mizukami et al., 2017).

Category	Parameters	Unit	Related parameters and description	Feasible range	
				Lower	Upper
g-parameters	g1	−	Total depth	0.1	4.0
	g2, g3	−	The number of the top two soil layers in the CONUS 11-layer soil profile	1, 4	3, 9
	g4, g5	−	b_{infilt}, variable infiltration curve parameter	−2.0, 0.8	1.0, 1.2
	g6, g7, g8	−	K_S, saturated hydrologic conductivity	−0.66, 0.0113, −0.0070	−0.54, 0.0139, −0.0058
	g9, g10, g11	−	phis, saturated water content	45.5, −0.3, −0.1	55.5, −0.01, −0.01
	g12, g13, g14	−	psis, saturation matric potential	1.0, −0.01, 0.006	2.0, −0.009, 0.0066
	g15, g16, g17	−	b, the slope of Campbell's retention curve in log space	2.5, 0.1, −0.005	3.6, 0.2, −0.001
	g18, g19	−	expt, the exponent in Campbell's equation for hydraulic conductivity	2.8, 1.5	3.2, 2.5
	g20	−	*FC*, field capacity	0.8	1.2
	g21	−	D4	1.5	2.5
	g22	−	D1	1.75	3.5
	g23	−	D2	1.75	3.5
	g24	−	D3	0.001	2.0
	g25	−	dp, soil thermal damping depth	0.9	1.1
	g26, g27	−	bubble, bubbling pressure of soil	0.1, 0.0	0.8, 10.0
	g28	−	quartz, quartz content of soil	0.7	0.9
	g29	−	bd, bulk density of soil layer	0.9	1.1
	g30, g31, g32	−	sd, soil particle density	0.9, 0.9, 0.9	1.1, 1.1, 1.1
	g33	−	Wcr_FRACT, fractional soil moisture content at the critical point	0.8	1.2
	g34	−	*WP*, wilting point	0.8	1.2
	g35	−	Wpwp_FRACT, fractional soil moisture content at the wilting point	0.8	1.2
	g36	−	rough, surface roughness of bare soil	0.9	1.1
	g37	−	snow rough, surface roughness of snowpack	0.9	1.1
UH parameters	tp	[h]	Time of peak occurrence	1.0	24.0
	μ	[h^{-1}]	Rising coefficient	2.0	10.0
	m	−	Recessing coefficient	0.5	6.0
Routing parameters	g38, g39, g40	−	*v*, Flow velocity	0.01, 0.1, 0.2	0.5. 0.3, 0.4
	g41	−	*D*, Flow diffusivity	0.01	0.5

https://doi.org/10.5194/egusphere-2026-4655
Preprint. Discussion started: 12 August 2026

Table A2. Simplified set of 15 free parameters for calibration.

Category	Parameters	Unit	Related parameters and description	Feasible range	
				Lower	Upper
g-parameters	g1	–	Total depth	0.1	4.0
	g2, g3	–	The number of the top two soil layers in the CONUS 11-layer soil profile	1, 4	3, 9
	g4, g5	–	b_{infilt}, variable infiltration curve parameter	−2.0, 0.8	1.0, 1.2
	g6	–	D1	1.75	3.5
	g7	–	D2	1.75	3.5
	g8	–	D3	0.001	2.0
UH parameters	t_p	[h]	Time of peak occurrence	1.0	24.0
	μ	[h^{-1}]	Rising coefficient	2.0	10.0
	m	–	Recessing coefficient	0.5	6.0
Routing parameters	g9, g10, g11	–	v, Flow velocity	0.01, 0.1, 0.2	0.5, 0.3, 0.4
	g12	–	D, Flow diffusivity	0.01	0.5

615 **Appendix B Model calibration process under single and multiple objective settings**

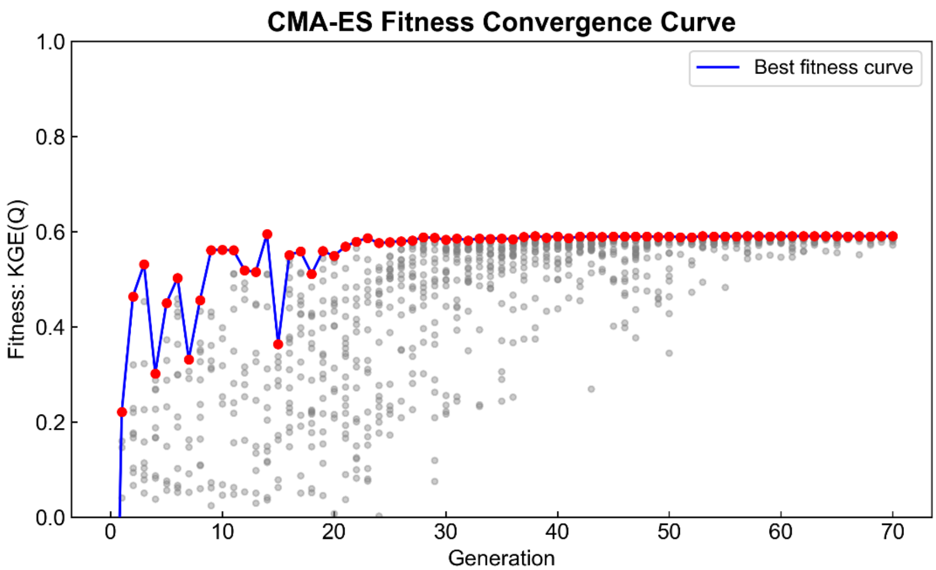

Figure. B1. Convergence curve obtained from the single-objective calibration for Basin Setup A, with the Kling–Gupta efficiency (KGE) of streamflow (Q) as the objective. The maximum fitness shows convergence after around 20 generations, whereas population-level convergence is observed after approximately 50 generations.

https://doi.org/10.5194/egusphere-2026-4655
Preprint. Discussion started: 12 August 2026

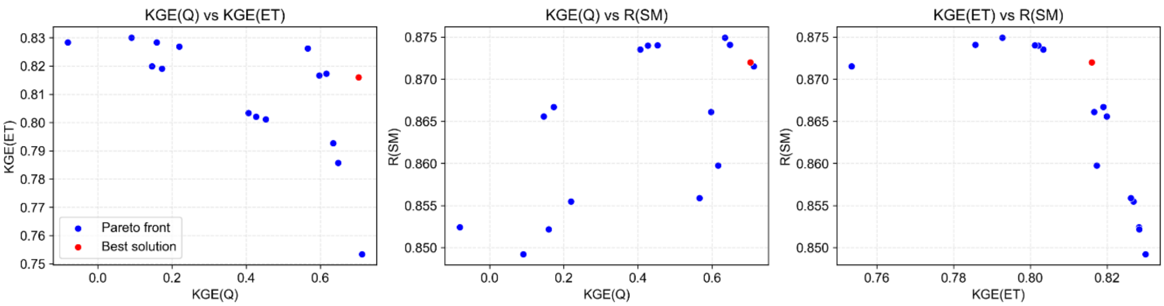

Figure. B2. Pareto front curves obtained from the multi-objective calibration for Basin Setup B, with three objectives including the Kling–Gupta efficiency (KGE) of streamflow (Q), the KGE of actual evapotranspiration (ET), and the correlation coefficient (R) of standardized soil moisture (SM). A certain degree of trade-off is observed between KGE (ET) and KGE (Q) as well as KGE (ET) and KGE (SM), while KGE (Q) and R (SM) tend to show a more synergistic behaviour.

Appendix C Model calibration process under single and multiple objective settings

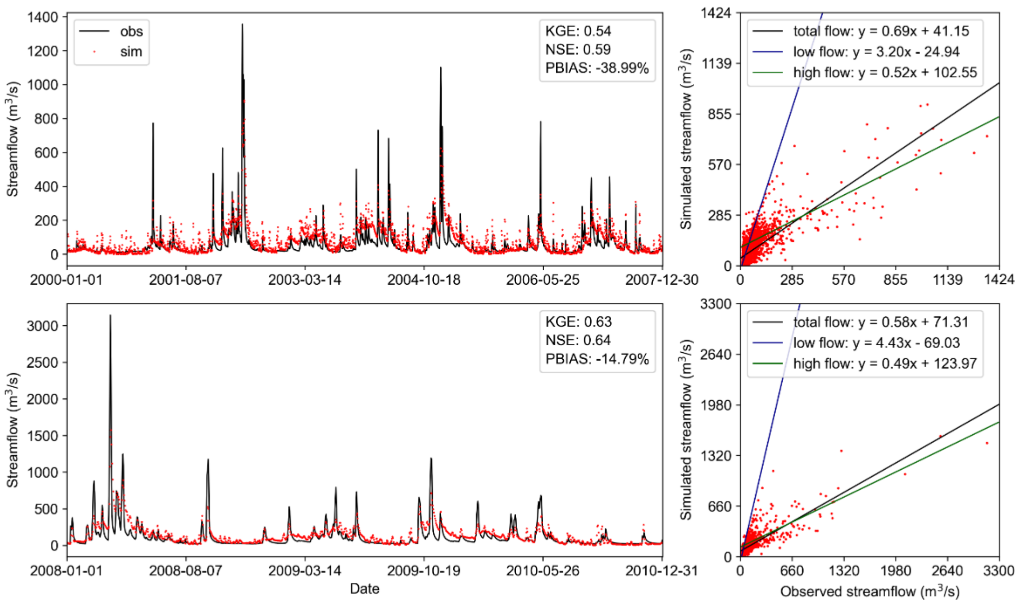

Figure. C1. Comparison of daily simulated streamflow from the 8 km-resolution VIC model against observations during the calibration period (top two panels) and validation period (bottom two panels). Low-flow and high-flow thresholds are defined as the 30th and 70th percentiles of the total flow range, respectively.

https://doi.org/10.5194/egusphere-2026-4655
Preprint. Discussion started: 12 August 2026

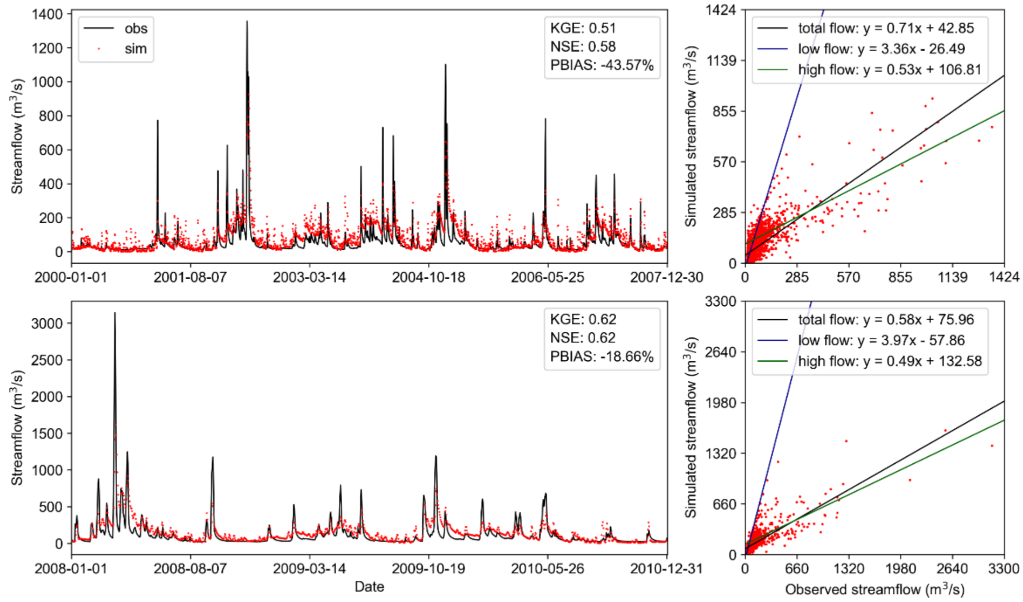

Figure. C2. Comparison of daily simulated streamflow from the 6 km-resolution VIC model against observations during the calibration period (top two panels) and validation period (bottom two panels). Low-flow and high-flow thresholds are defined as the 30th and 70th percentiles of the total flow range, respectively.

Code and data availability

The source code of Easy VIC Build (EVB) used in this study (EVB v1.0.0) is archived in Zenodo and is available at https://doi.org/10.5281/zenodo.21738705 (Zheng et al., 2026b). The primary datasets associated with this study, including the modelling files for the Gasconade River Basin (GRB) and Jing River Basin (JRB) case studies, are archived in Zenodo and are available at https://doi.org/10.5281/zenodo.21771543 (Zheng, 2026c). All datasets used in this study are publicly available through open-source platforms. The basin characteristics and daily runoff records were obtained from the Catchment Attributes and Meteorology for Large-sample Studies (CAMELS) dataset (Addor et al., 2017), accessible at https://ncar.github.io/hydrology/datasets/CAMELS_attributes. The NLDAS-2 forcing product (Xia et al., 2009; Xia et al., 2012) is available at the NASA Goddard Earth Sciences Data and Information Services Center (GES DISC) (https://disc.gsfc.nasa.gov/datasets/NLDAS_FORA0125_H_002/summary), while the CONUS-SOIL dataset (Miller and White, 1998) can be accessed at http://www.soilinfo.psu.edu/. Topographic data were derived from the STRM DEM dataset (Jarvis et al., 2008), available at http://srtm.csi.cgiar.org/srtmdata/, and land cover information was obtained from the UMD Land Cover product (Hansen et al., 2021), accessible at https://iridl.ldeo.columbia.edu/SOURCES/.UMD/.GLCF/.GLCDS/. Remote sensing data from MODIS, including MCD43D51.061 BSA (Schaaf and Wang, 2021), MOD13A3.061 NDVI (Didan, 2021), and MOD15A2H.061 LAI (Myneni et al., 2021), were downloaded from the Land Processes Distributed Active Archive Center (LP DAAC) (https://lpdaac.usgs.gov/). Additionally, soil temperature data were obtained from the

ERA5 Land dataset (Muñoz Sabater, 2019), available at https://cds.climate.copernicus.eu/datasets/reanalysis-era5-land-monthly-means. The SoilGrids1km dataset is publicly available from the official website: https://soilgrids.org (Poggio et al., 2021). The CMFD and Soil Hydraulic Parameters for China datasets are provided by National Tibetan Plateau / Third Pole Environment Data Center (http://data.tpdc.ac.cn).

Author contributions

XZ: Conceptualization, Methodology, Software, Writing – original draft, Writing – review & editing, Visualization. **DL**: Conceptualization, Methodology, Writing – review & editing, Funding acquisition. **QT**: Writing – review & editing. **QL**: Validation. **HL**: Validation. **HW**: Supervision.

Competing interests

The authors declare that they have no conflicts of interest.

Acknowledgements

This study was performed as part of the PhD project of Xudong Zheng and financially supported by the National Key R&D Program of China [Grant No. 2022YFF1302200] and National Natural Science Foundation of China [Grant No. 52279025].

Financial support

This study is financially supported by the National Key R&D Program of China [Grant No. 2022YFF1302200] and National Natural Science Foundation of China [Grant No. 52279025].

https://doi.org/10.5194/egusphere-2026-4655
Preprint. Discussion started: 12 August 2026

References

Addor, N., Newman, A. J., Mizukami, N., and Clark, M. P.: The CAMELS data set: catchment attributes and meteorology for large-sample studies, Hydrology and Earth System Sciences, 21, 5293-5313, 10.5194/hess-21-5293-2017, 2017.

Ahrens, C. D.: Meteorology today: an introduction to weather, climate, and the environment, Cengage Learning Canada Inc2015.

Andréassian, V. et al. Crash tests for a standardized evaluation of hydrological models. Hydrology and Earth System Sciences, 13: 1757-1764, 2009.

Beven, K.: Towards an Alternative Blueprint for a Physically Based Digitally Simulated Hydrologic Response Modelling System, Hydrological Processes - HYDROL PROCESS, 16, 189-206, 10.1002/hyp.343, 2002.

Beven, K.: A brief history of information and disinformation in hydrological data and the impact on the evaluation of hydrological models. Hydrological Sciences Journal, 69(5): 519-527. DOI:10.1080/02626667.2024.2332616, 2024.

Bohn, T. J. and Vivoni, E. R.: MOD-LSP, MODIS-based parameters for hydrologic modelling of North American land cover change, Scientific Data, 6, ARTN 14410.1038/s41597-019-0150-2, 2019.

Broman, D., Voisin, N., Kao, S.-C., Fernandez, A., and Ghimire, G.: Multi-scale impacts of climate change on hydropower for long-term water-energy planning in the contiguous United States, Environmental Research Letters, 19, 10.1088/1748-9326/ad6ceb, 2024.

Carvalho, V.S.O. et al. Assessment of land use changes in the Verde River basin using two hydrological models. J S Am Earth Sci, 118: 103954. DOI:https://doi.org/10.1016/j.jsames.2022.103954, 2022.

Chagas, V., P. Chaffe, and G. Blöschl (2024), Regional Low Flow Hydrology: Model Development and Evaluation, Water Resources Research, 60.

Chen, Y., Shi, P., Ji, X., Qu, S., Zhao, L., and Dong, F.: New method to calculate the dynamic factor–flow velocity in Geomorphologic instantaneous unit hydrograph, Scientific Reports, 9, 10.1038/s41598-019-50723-x, 2019.

Cortés-Salazar, N., Vasquez, N., Mizukami, N., Mendoza, P., and Vargas, X.: To what extent does river routing matter in hydrological modelling?, Hydrology and Earth System Sciences, 27, 3505-3524, 10.5194/hess-27-3505-2023, 2023.

Cosby Jr, B., Hornberger, G., Clapp, R., Ginn, T. A Statistical Exploration of Relationships of Soil Moisture Characteristics to the Physical Properties of Soils. Water Resources Research - WATER RESOUR RES, 20: 682-690. DOI:10.1029/WR020i006p00682, 1984.

da Costa-Luis, C.: tqdm: A Fast, Extensible Progress Meter for Python and CLI, Journal of Open Source Software, 4, 1277, 10.21105/joss.01277, 2019.

Dai, Y., W. Shangguan, Q. Duan, B. Liu, S. Fu, G. Niu, (2013). Development of a China Dataset of Soil Hydraulic Parameters Using Pedotransfer Functions for Land Surface Modelling. Journal of Hydrometeorology, doi: 10.1175/JHM-D-12-0149.1.

https://doi.org/10.5194/egusphere-2026-4655
Preprint. Discussion started: 12 August 2026

Deb, K., Pratap, A., Agarwal, S., and Meyarivan, T.: A fast and elitist multiobjective genetic algorithm: NSGA-II, IEEE Trans. on Evol, IEEE Transactions on Evolutionary Computation - TEC, 6, 2002.

Didan, K.: MODIS/Terra Vegetation Indices Monthly L3 Global 1km SIN Grid V061 (V061) [dataset], 10.5067/MODIS/MOD13A3.061, 2021.

Duan, Q. et al. Model Parameter Estimation Experiment (MOPEX): Overview and Summary of the Second and Third Workshop Results. 320, 2005.

Fortin, F.-A., De Rainville, F.-M., Gardner, M. A., Parizeau, M., and Gagné, C.: DEAP: Evolutionary algorithms made easy, Journal of Machine Learning Research, Machine Learning Open Source Software, 13, 2171-2175, 2012.

Koch, J., Jensen, K., Stisen, S. Toward a true spatial model evaluation in distributed hydrological modelling: Kappa statistics, Fuzzy theory, and EOF analysis benchmarked by the human perception and evaluated against a modelling case study. Water Resources Research, 51. DOI:10.1002/2014WR016607, 2015.

Gamma, Erich, Helm, Richard, Johnson, R., Ralph, Vlissides, and John: Design Patterns: Elements of Reusable Object-Oriented Software, 10.1081/E-ESE-120044217, 1995.

Gillies, S.: Rasterio: geospatial raster I/O for (Yu et al.) programmers, Mapbox [code], 2013.

Gou, J., Miao, C., Duan, Q., Tang, Q., di, Z., Liao, W., Wu, J., and Zhou, R.: Sensitivity analysis ‐ based automatic parameter calibration of the variable infiltration capacity (VIC) model for streamflow simulations over China, Water Resources Research, 56, 10.1029/2019WR025968, 2020.

Gou, J., Miao, C., Samaniego, L., Xiao, M., Wu, J., and Guo, X.: CNRD v1.0: A High-Quality Natural Runoff Dataset for Hydrological and Climate Studies in China, Bulletin of the American Meteorological Society, 102, E929-E947, 10.1175/BAMS-D-20-0094.1, 2021.

Guo, J.: General and Analytic Unit Hydrograph and Its Applications, Journal of Hydrologic Engineering, 27, 10.1061/(ASCE)HE.1943-5584.0002149, 2022a.

Guo, J. K.: General Unit Hydrograph from Chow's Linear Theory of Hydrologic Systems and Its Applications, Journal of Hydrologic Engineering, 27, Artn 0402202010.1061/(Asce)He.1943-5584.0002184, 2022b.Gupta, H., Kling, H., Yilmaz, K., Martinez, G. Decomposition of the Mean Squared Error and NSE Performance Criteria: Implications for Improving Hydrological Modelling. Journal of Hydrology, 377: 80-91. DOI:10.1016/j.jhydrol.2009.08.003, 2009.

Gupta, H., Kling, H., Yilmaz, K., and Martinez, G.: Decomposition of the Mean Squared Error and NSE Performance Criteria: Implications for Improving Hydrological Modelling, Journal of Hydrology, 377, 80-91, 10.1016/j.jhydrol.2009.08.003, 2009.

Gupta, H., Perrin, C., Blöschl, G., Montanari, A., Kumar, R., Clark, M., and Andréassian, V.: Large-sample hydrology: a need to balance depth with breadth, Hydrology and Earth System Sciences, 18, 10.5194/hess-18-463-2014, 2014.

Hamman, J., Nijssen, B., Bohn, T., Gergel, D., and Mao, Y.: The Variable Infiltration Capacity model version 5 (VIC-5): infrastructure improvements for new applications and reproducibility, Geosci Model Dev, 11, 3481-3496, 10.5194/gmd-11-3481-2018, 2018.

Hansen, M., Defries, R., Townshend, J., and Sohlberg, R.: Global land cover classification at 1km resolution using a decision tree classifier, J Remote Sens, 2021.

Hansen, N. and Ostermeier, A.: Completely Derandomized Self-Adaptation in Evolution Strategies, Evolutionary Computation, 9, 159-195, 10.1162/106365601750190398, 2001.

Harris, C., Millman, K., Walt, S., Gommers, R., Virtanen, P., Cournapeau, D., Wieser, E., Taylor, J., Berg, S., Smith, N., Kern, R., Picus, M., Hoyer, S., Kerkwijk, M., Brett, M., Haldane, A., Río, J., Wiebe, M., Peterson, P., and Oliphant, T.: Array programming with NumPy, Nature, 585, 357-362, 10.1038/s41586-020-2649-2, 2020.

He, J. et al. The first high-resolution meteorological forcing dataset for land process studies over China. Sci Data, 7(1): 25. DOI:10.1038/s41597-020-0369-y, 2020.

Hengl, T. et al. SoilGrids1km — Global Soil Information Based on Automated Mapping. Plos One, 9: e105992. DOI: 10.1371/journal.pone.0105992, 2014.

Hoyer, S. and Hamman, J.: xarray: N-D labeled Arrays and Datasets in Python, Journal of Open Research Software, 5, 10.5334/jors.148, 2017.

Hunter, J.: Matplotlib: A 2D Graphics Environment, Comput Sci Eng, 9, 90-95, 10.1109/MCSE.2007.55, 2007.

Jarvis, A., Reuter, H., Nelson, A., and Guevara, E.: Hole-filled seamless SRTM data V4. Tech. rep., International Centre for Tropical Agriculture (CIAT), Cali, Columbia, 2008.

Jia, X., Shao, M.a., Zhang, C., Zhao, C., 2015. Regional temporal persistence of dried soil layer along south-north transect of the Loess Plateau, China. Journal of Hydrology, 528. DOI:10.1016/j.jhydrol.2015.06.025.

Jordahl, K., Bossche, J. V. d., Fleischmann, M., Wasserman, J., McBride, J., Gerard, J., Tratner, J., Perry, M., Badaracco, A. G., Farmer, C., Hjelle, G. A., Snow, A. D., Cochran, M., Gillies, S., Culbertson, L., Bartos, M., Eubank, N., maxalbert, Bilogur, A., Rey, S., Ren, C., Arribas-Bel, D., Wasser, L., Wolf, L. J., Journois, M., Wilson, J., Greenhall, A., Holdgraf, C., Filipe, and Leblanc, F.: geopandas/geopandas: v0.14.4 (v0.14.4), Zenodo [code], 10.5281/zenodo.3946761, 2020.

Lehmann, F., Vishwakarma, B., Bamber, J. How well are we able to close the water budget at the global scale? Hydrology and Earth System Sciences, 26: 35-54. DOI:10.5194/hess-26-35-2022, 2022.

Lindsay, J. and Wu, Q.: Whitebox Workflows for Python (v1.0) [code], 2021.

Liu, D., Tian, F., Hu, H., and Hu, H.: The role of run-on for overland flow and the characteristics of runoff generation in the Loess Plateau, China, Hydrological Sciences Journal-journal Des Sciences Hydrologiques - HYDROLOG SCI J, 57, 1-11, 10.1080/02626667.2012.695870, 2012a.

Liu, Y., Weerts, A., Clark, M., Franssen, H.-J., Kumar, S., Hamid, M., Seo, D.-J., Schwanenberg, D., Smith, P., van Dijk, A., Velzen, N., He, M., Lee, H., Noh, S. J., Rakovec, O., and Restrepo, P.: Advancing data assimilation in operational hydrologic forecasting: Progresses, challenges, and emerging opportunities, Hydrology and Earth System Sciences, 16, 10.5194/hess-16-3863-2012, 2012b.

Lehmann, F., Vishwakarma, B., Bamber, J. How well are we able to close the water budget at the global scale? Hydrology and Earth System Sciences, 26: 35-54. DOI:10.5194/hess-26-35-2022, 2022.

https://doi.org/10.5194/egusphere-2026-4655
Preprint. Discussion started: 12 August 2026

Lohmann, D., Nolte-Holube, R., and Raschke, E.: A large-scale horizontal routing model to be coupled to land surface parametrization schemes, Tellus, Series A: Dynamic Meteorology and Oceanography, 48, 708-721, 10.3402/tellusa.v48i5.12200, 1996.

McKinney, W.: pandas: a Foundational Python Library for Data Analysis and Statistics, Python High Performance Science Computer, 2011.

McKay, M., Beckman, R., Conover, W. A Comparison of Three Methods for Selecting Values of Input Variables in the Analysis of Output from a Computer Code. Technometrics, 21: 239-245. DOI:10.2307/1268522, 1979.

Martens, B. et al. GLEAM v3: Satellite-based land evaporation and root-zone soil moisture. Geosci Model Dev, 10. DOI:10.5194/gmd-10-1903-2017, 2017.

Mei, Y., Mai, J., Do, H., Gronewold, A., Reeves, H., Eberts, S., Niswonger, R., Regan, R., and Hunt, R.: Can Hydrological Models Benefit From Using Global Soil Moisture, Evapotranspiration, and Runoff Products as Calibration Targets?, Water Resources Research, 59, 10.1029/2022WR032064, 2023.Miller, D. and White, R.: A Conterminous United States Multilayer Soil Characteristics Dataset for Regional Climate and Hydrology Modelling, Earth Interactions - EARTH INTERACT, 2, 2-2, 10.1175/1087-3562(1998)002<0001:ACUSMS>2.3.CO;2, 1998.

Miao, Y. and Wang, A.: A daily 0.25°×0.25° hydrologically based land surface flux dataset for conterminous China, 1961-2017, Journal of Hydrology, 590, 125413, 10.1016/j.jhydrol.2020.125413, 2020.

Mizukami, N., Clark, M., Newman, A., Wood, A., Gutmann, E., Nijssen, B., Rakovec, O., and Samaniego, L.: Toward seamless large domain parameter estimation for hydrologic models, Water Resources Research, 53, 10.1002/2017wr020401, 2017.

Mizukami, N. et al. On the choice of calibration metrics for "high-flow" estimation using hydrologic models. Hydrology and Earth System Sciences, 23(6): 2601-2614. DOI:10.5194/hess-23-2601-2019, 2019.

Muñoz Sabater, J.: ERA5-Land monthly averaged data from 1950 to present [dataset], 10.24381/cds.68d2bb30, 2019.

Myneni, R., Knyazikhin, Y., and Park, T.: MODIS/Terra Leaf Area Index/FPAR 8-Day L4 Global 500m SIN Grid V061 (V061) [dataset], 10.5067/MODIS/MOD15A2H.061, 2021.

Newman, A. J., Clark, M. P., Sampson, K., Wood, A., Hay, L. E., Bock, A., Viger, R. J., Blodgett, D., Brekke, L., Arnold, J. R., Hopson, T., and Duan, Q.: Development of a large-sample watershed-scale hydrometeorological data set for the contiguous USA: data set characteristics and assessment of regional variability in hydrologic model performance, Hydrology and Earth System Sciences, 19, 209-223, 10.5194/hess-19-209-2015, 2015.

Office, M.: Cartopy: a cartographic python library with a Matplotlib interface, 2010-2015.

Peters-Lidard, C., Clark, M., Samaniego, L., Verhoest, N., van Emmerik, T., Uijlenhoet, R., Achieng, K., Franz, T., and Woods, R.: Scaling, Similarity, and the Fourth Paradigm for Hydrology, Hydrology and Earth System Sciences, 21, 3701-3713, 10.5194/hess-21-3701-2017, 2017.

Poggio, L. et al. SoilGrids 2.0: producing soil information for the globe with quantified spatial uncertainty. Soil-Germany, 7: 217-240. DOI:10.5194/soil-7-217-2021, 2021.

https://doi.org/10.5194/egusphere-2026-4655
Preprint. Discussion started: 12 August 2026

Qiu, L., Wu, Y., Wang, L., Lei, X., Liao, W., Hui, Y., and Meng, X.: Spatiotemporal response of the water cycle to land use conversions in a typical hilly–gully basin on the Loess Plateau, China, Hydrology and Earth System Sciences, 21, 6485-6499, 10.5194/hess-21-6485-2017, 2017.

Rakovec, O., Kumar, R., Attinger, S., and Samaniego, L.: Improving the realism of hydrologic model functioning through multivariate parameter estimation, Water Resources Research, 52, 10.1002/2016WR019430, 2016.

Rew, R. and Davis, G.: NetCDF: An interface for scientific data access, Computer Graphics and Applications, IEEE, 10, 76-82, 10.1109/38.56302, 1990.

Samaniego, L., Kumar, R., and Attinger, S.: Multiscale parameter regionalization of a grid-based hydrologic model at the mesoscale, Water Resour. Res., 46, 10.1029/2008WR007327, 2010.

Schaaf, C. and Wang, Z.: MODIS/Terra+Aqua BRDF/Albedo Black Sky Albedo Shortwave Daily L3 Global 30ArcSec CMG V061 (V061) [dataset], 10.5067/MODIS/MCD43D51.061, 2021.

Sherman, L.: Stream Flow from Rainfall by the Unit-Graph Method, Eng. News-Record., 108, 1932.

Singh, S., Pahlow, M., Booker, D., Shankar, U., and Chamorro, A.: Towards baseflow index characterisation at national scale in New Zealand, Journal of Hydrology, 568, 10.1016/j.jhydrol.2018.11.025, 2018.

Sun, R., Duan, Q., and Huo, X.: Multi‐Objective Adaptive Surrogate Modelling‐Based Optimization for Distributed Environmental Models Based on Grid Sampling, Water Resources Research, 57, 10.1029/2020WR028740, 2021.

Sun, R., Pan, B., and Duan, Q.: A surrogate modelling method for distributed land surface hydrological models based on deep learning, Journal of Hydrology, 624, 129944, 10.1016/j.jhydrol.2023.129944, 2023.

Széles, B., Parajka, J., Hogan, P., Silasari, R., Pavlin, L., Strauss, P., and Blöschl, G.: The Added Value of Different Data Types for Calibrating and Testing a Hydrologic Model in a Small Catchment, Water resources research, 56, e2019WR026153, 10.1029/2019WR026153, 2020.

Todini, E.: History and perspectives of hydrological catchment modelling, Hydrol Res, 42, 73-85, 2011.

Virtanen, P., Gommers, R., Oliphant, T., Haberland, M., Reddy, T., Cournapeau, D., Burovski, E., Peterson, P., Weckesser, W., Bright, J., Walt, S., Brett, M., Wilson, J., Millman, K., Mayorov, N., Nelson, A., Jones, E., Kern, R., Larson, E., and Vázquez-Baeza, Y.: SciPy 1.0: fundamental algorithms for scientific computing in Python, Nature Methods, 17, 1-12, 10.1038/s41592-019-0686-2, 2020.

Wambura, F.J., Dietrich, O., Lischeid, G. Improving a distributed hydrological model using evapotranspiration-related boundary conditions as additional constraints in a data-scarce river basin. Hydrol Process, 32(6): 759-775, 2018.

Wang, Z., Vivoni, E., Whitney, K., Xiao, M., and Mascaro, G.: On the Sensitivity of Future Hydrology in the Colorado River to the Selection of the Precipitation Partitioning Method, Water Resources Research, 60, 10.1029/2023WR035801, 2024b.Wen, Z., Liang, X., and Yang, S.: A new multiscale routing framework and its evaluation for land surface modelling applications, Water Resources Research, 48, 8528, 10.1029/2011WR011337, 2012.

https://doi.org/10.5194/egusphere-2026-4655
Preprint. Discussion started: 12 August 2026

Wenger, S.J., Luce, C.H., Hamlet, A.F., Isaak, D.J., Neville, H.M., 2010. Macroscale hydrologic modelling of ecologically relevant flow metrics. Water Resources Research, 46. DOI:Artn W0951310.1029/2009wr008839

Wi, S., Ray, P., Demaria, E. M. C., Steinschneider, S., and Brown, C.: A user-friendly software package for VIC hydrologic model development, Environmental Modelling & Software, 98, 35-53, 10.1016/j.envsoft.2017.09.006, 2017.

Xia, Y., NCEP/EMC, and Mocko, D. (Ed.): NLDAS Primary Forcing Data L4 Hourly 0.125° × 0.125° V002 [data set], NASA Goddard Earth Sciences Data and Information Services Center (GES DISC), Greenbelt, Maryland, USA, 10.5067/6J5LHHOHZHN4, accessed: 24 May 2024, 2009.Xia, Y., Mitchell, K., Ek, M., Sheffield, J., Brian, C., Wood, E., Luo, L., Alonge, C., Wei, H., Meng, J., Livneh, B., Lettenmaier, D., Koren, V., Duan, Q., Mo, K., Fan, Y., and Mocko, D.: Continental-Scale Water and Energy Flux Analysis and Validation for the North American Land Data Assimilation System Project Phase 2 (NLDAS-2): 1. Intercomparison and Application of Model Products, Journal of Geophysical Research (Atmospheres), 117, 3109, 10.1029/2011JD016048, 2012.

Yan, H., Sun, N., Eldardiry, H., Thurber, T., Reed, P., Malek, K., Gupta, R., Kennedy, D., Swenson, S., Hou, Z., Cheng, Y., and Rice, J.: Large Ensemble Diagnostic Evaluation of Hydrologic Parameter Uncertainty in the Community Land Model Version 5 (CLM5), Journal of Advances in Modelling Earth Systems, 15, 10.1029/2022MS003312, 2023.

Yang, Y., Endreny, T. A., and Nowak, D. J. J. J. o. E. s.: Application of advection-diffusion routing model to flood wave propagation: A case study on Big Piney River, Missouri USA, 27, 9-14, 2016.

Yeste, P., García-Valdecasas Ojeda, M., Gámiz-Fortis, S. R., Castro-Díez, Y., Bronstert, A., and Esteban-Parra, M. J.: A large-sample modelling approach towards integrating streamflow and evaporation data for the Spanish catchments, Hydrol. Earth Syst. Sci., 28, 5331-5352, 10.5194/hess-28-5331-2024, 2024.

Zacharias, S. et al. A Network of Terrestrial Environmental Observatories in Germany. Vadose Zone J, 10: 955-973. DOI:10.2136/vzj2010.0139, 2011.

Zhang, Z., Chen, Y., Zhang, G., Zhang, X., 2023. Simulation of Hydrological Processes in the Jing River Basin Based on the WEP Model. Water-Sui, 15: 2989. DOI:10.3390/w15162989.

Zheng, X., Liu, D., Wang, H., Ma, C., Liu, H., Ming, G., Li, Q., Khan, M. Y. A., and Hussain, F.: What can hydrological modelling gain from spatially explicit parameterization and multi-gauge calibration?, Hydrol. Earth Syst. Sci., 30, 2493-2521, 10.5194/hess-30-2493-2026, 2026.

Zheng, X. Easy VIC Build v0.2.0 [Computer software]. Zenodo, https://doi.org/10.5281/zenodo.21738705, 2026.

Zheng, X. Data for "An Open-Source Python Framework for the Flexible Deployment and Advanced Applications of the Variable Infiltration Capacity (VIC) Model" [Dataset]. Zenodo, https://doi.org/10.5281/zenodo.21771543, 2026.

Zhong, L., Lei, H., Gao, B. Developing a Physics - Informed Deep Learning Model to Simulate Runoff Response to Climate Change in Alpine Catchments. Water Resources Research, 59(6). DOI:10.1029/2022wr034118, 2023.

Zink, M., Kumar, R., Cuntz, M., and Samaniego, L.: A high-resolution dataset of water fluxes and states for Germany accounting for parametric uncertainty, Hydrology and Earth System Sciences, 21, 1769-1790, 10.5194/hess-21-1769-2017, 2017.